ACCEPTED MANUSCRIPT
Journal of Renewable and Sustainable Energy
AIP Publishing
This is the author's peer reviewed, accepted manuscript. However, the online version of record will be different from this version once it has been copyedited and typeset.
PLEASE CITE THIS ARTICLE AS DOI: 10.1063/5.0125713

Accepted to J. Renew. Sustain. Energy 10.1063/5.0125713

Implementation of an enhanced M5p tree controller based on ANN Data applied to doubly-fed induction generator

M. Hallouz,[1] N. Kabeche,[1] S. Moulahoum,[1] and R. Benkercha[1]
Laboratory of Electrical Engineering & Automatic, University of Medea, Algeria

(*Electronic mail: kabache.nadir@univ-medea.dz.)

(Dated: 23 November 2022)

The present paper concerns the indirect control of the stator powers of a wind system based on a doubly-fed induction generator (DFIG). The DFIG is controlled by its rotor through an association of a grid side converter (GSC) with a rotor side converter (RSC) and the stator makes it possible to supply a resistive load. The current 1.5kw generator is driven by a wind emulator based on a DC motor. Simulation and experimental studies are carried out using first, a conventional PI, an neural network controller (NNC), and then a M5P decision tree algorithm (M5P-DTA) is proposed to bring improvements to the control. The M5P-DTA is obtained from a learning process via the data set provided by neural network controllers. The proposed algorithm allows a fast and less complex control scheme for the DFIG. The simulation study and its results are obtained through the MATLAB/SIMULINK software, while the experimental test is carried out via the dSPACE DS1104 interface card ordered by MATLAB and the graphical interface of the Control-Desk software.

I. INTRODUCTION

Wind energy has developed through advances in wind technology, above all the introduction of the DFIG. Through the variable-speed opportunity, the DFIG allows extracting and converting the largest part of available wind energy. DFIG has been incorporated in most wind energy conversion systems worldwide. DFIG's management in the wind power sector has undergone more changes and improvements, where several control strategies are employed whose common objective is to improve the dynamic performances of the generator via the control of its the active and reactive powers ([1–4]).

Since the DFIG is a nonlinear system, the control task cannot be performed easily and directly. To make things easier, the field-oriented principle has been introduced to achieve the decoupling between magnetically (reactive power) and mechanical (active power) behaviors allowing therefore a separate and independent control for each variable. In literature, several studies and diagrams have been conducted for DFIG control. The conventional PI controllers offers generally the easy way for the active and reactive power control[5]. Despite their synthesis simplicity they give less satisfactory performances and suffer from dependency on system parameters. In ([6,7]), the authors propose a direct power control (DPC) based on the switching sequences table to produce a robust and fast power response. However, this technique has the drawback of the variable switching frequency[8]. To fix this problem, a standard PI combined with DPC-space vector modulation has been proposed in ([9,10]). In ([11]) a nonlinear approaches based on the sliding mode control (SMC) is considered, however, the use of the first-order SMC induces the chattering phenomenon. In ([12,13]), the authors combined a standard PI with the SMC to improve the robustness of the control and attenuate reduce the chattering effect. In an attempt to fix the chattering problem a second-order SMC is proposed in ([14,15]). Beside, other non-linear approaches were applied on the DFIG such as the Lyapunov based backstepping control[16], The association of the super torsion SMC strategy with the DPC strategy ([17]), the association of the DPC with an ANFIS (adaptive neuro-fuzzy inference system) and a super twisting SMC ([18]). Despite their quite satisfactory results, these approaches are very expensive in terms of time and difficult to implement, especially for non-linear ones.

Therefore, it was interesting to resort to artificial intelligent solutions to further improve the DFIG performances. Some attempts based on fuzzy logic controllers (FLC) have been introduced to substitute the standard PI in ([19–21]). The required improvement needs to increase the FLC membership, which leads to more difficulty in experimental implementation. The use of NNC in ([22–24]) shows that they are fast, simple, and allow avoiding the drawback of system parameters variation via the learning features. In the paper ([25]), the author uses an ANFIS system thus taking advantage of both FLC robustness and ANN flexibility. However, the approximation error may arise from insufficient learning, having less number of hidden units or insufficient training data. Moreover, the implementation of the FCL need more space on target board, so we must use look-up table blocks to replace FLC sub-blocks.

Moreover, several evolutionary algorithms appeared in the last decades such as genetic algorithms, particle swarm optimization, ant colony optimization, and M5P decision tree algorithms (M5P-DTA). The M5P-DTA combines the features of classification and linear regression. Like piecewise linear functions, it fits system data into a multivariate linear model so that the nonlinear relationship of the data sets is approximated. Compared to neural networks, the M5P-DTA has the same accuracy with the same data but learns efficiently and faster for very big data sets. In addition, the implementation of M5P-DTA is easy and does not need complex computations.

Even if the M5P-DTA has been introduced in some photovoltaic-based renewable energy systems application it stays new and unknown for wind energy conversion systems control. Therefore, in this paper, the M5P-DTA is used for the indirect control of the active and reactive powers of the DFIG. The training data contained several inputs-outputs set collected from the DFIG through two NNC where rotor cur-

ACCEPTED MANUSCRIPT
Journal of Renewable and Sustainable Energy
AIP Publishing
This is the author's peer reviewed, accepted manuscript. However, the online version of record will be different from this version once it has been copyedited and typeset.
PLEASE CITE THIS ARTICLE AS DOI: 10.1063/5.0125713

rents errors serve as inputs and rotor voltages as outputs. A comparison is performed between M5P-DTA and neural network controllers where this last was supported by an experimental test for both algorithms to prove the validity of the proposed approach. The major interest of this paper is to establish a control strategy less cumbersome, simple, and easy to realize.

The organisation of the paper begins with the modeling of the DFIG with the different proposed methods for the indirect control of the active and reactive powers of the DFIG stator. Then two NNC are proposed for the control of DFIG rotor currents. Thereafter and to give improvements in the DFIG control, the M5P-DTA has been proposed to substitute the two NNC for more accuracy and less computation time. Indeed, A learning data set has been recorded and used for the training to obtain a decision tree model, the training process is done by WEKA software. The obtained tree model is inserted in the control diagram instead of the two NNC. Finally, different tests, whether by simulation or by experimentation have been performed to validate the work presented here. For the experimental tests, they where achieved via MATLAB-SIMULINK software and a 1104 dSPACE cardboard.

II. MODELING OF THE WIND ENERGY CONVERSION SYSTEM

The addressed wind energy conversion system (WECS) shown in Fig. 1 consists of three parts: the wind turbine, the generator, and the load. For the turbine, a wind emulator based on a 1.5Kw Dc motor driven by a four quadrants Dc/Dc converter is proposed to simulate the real wind turbine behavior. The generator is a 1.5 Kw doubly-fed induction generator supplied by the rotor side Dc/Ac converter (RSC). The grid is connected with the system via the grid side Ac/Dc converter (GSC). The control of the DFIG, as mentioned above, will be carried out throw NNC and M5P-DTA algorithm. The control allows generating the switching signals for the rotor side converter. The load side consists of a resistive bank connected to the DFIG stator winding.

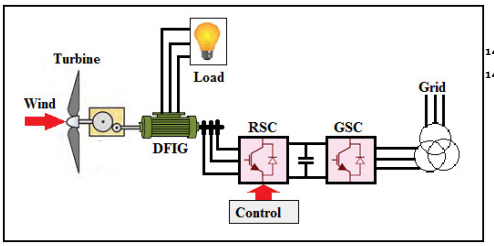


FIG. 1. Wind conversion system diagram.

The dynamical behaviour of the DFIG in the $d-$ and $q-axis$ (rotating frame) is represented by the following equations[26–30].

A. Stator and rotor voltages

$$V_{ds} = R_s I_{ds} + \frac{d\Phi_{ds}}{dt} - \omega_s \Phi_{qs}, \tag{1a}$$

$$V_{qs} = R_s I_{qs} + \frac{d\Phi_{qs}}{dt} + \omega_s \Phi_{ds}, \tag{1b}$$

$$V_{dr} = R_r I_{dr} + \frac{d\Phi_{dr}}{dt} - \omega_s \Phi_{qr}, \tag{1c}$$

$$V_{qr} = R_r I_{qr} + \frac{d\Phi_{qr}}{dt} + \omega_s \Phi_{dr}, \tag{1d}$$

B. Stator and rotor fluxes

$$\Phi_{ds} = L_s I_{ds} + L_m I_{dr}, \tag{2a}$$

$$\Phi_{qs} = L_s I_{qs} + L_m I_{qr}, \tag{2b}$$

$$\Phi_{dr} = L_r I_{dr} + L_m I_{ds}, \tag{2c}$$

$$\Phi_{qr} = L_r I_{qr} + L_m I_{qs}, \tag{2d}$$

C. Stator active and reactive powers

$$P_s = V_{ds} I_{ds} + V_{qs} I_{qs}, \tag{3a}$$

$$Q_s = V_{qs} I_{ds} - V_{ds} I_{qs}, \tag{3b}$$

Using Eqs. (1) and Eqs. (2) The dynamic of the DFIG can be organised as follows:

$$\begin{bmatrix} \frac{dI_{ds}}{dt} \\ \frac{dI_{qs}}{dt} \\ \frac{dI_{dr}}{dt} \\ \frac{dI_{qr}}{dt} \end{bmatrix} = A_1 \begin{bmatrix} I_{ds} \\ I_{qs} \end{bmatrix} + A_2 \begin{bmatrix} I_{dr} \\ I_{qr} \end{bmatrix} + A_3 \begin{bmatrix} V_{ds} \\ V_{qs} \\ V_{dr} \\ V_{qs} \end{bmatrix} \tag{4}$$

With,

$$A_1 = \begin{bmatrix} -R_s L_r & \omega_m L_m^2 - L_s L_r \sigma \omega_s \\ -\omega_m L_m^2 - L_s L_r \sigma \omega_s & -R_s L_r \\ R_s L_m & -\omega_m L_s L_m \\ \omega_m L_s L_m & R_s L_m \end{bmatrix} \tag{5}$$

ACCEPTED MANUSCRIPT
Journal of Renewable and Sustainable Energy
AIP Publishing
This is the author's peer reviewed, accepted manuscript. However, the online version of record will be different from this version once it has been copyedited and typeset.
PLEASE CITE THIS ARTICLE AS DOI: 10.1063/5.0125713

$$A_2 = \begin{bmatrix} R_r L_m & \omega_m L_r L_m \\ -\omega_m L_r L_m & R_r L_m \\ -R_r L_s & -\omega_m L_s L_r + L_s L_r \sigma \omega_s \\ \omega_m L_s L_r + L_s L_r \sigma \omega_s & -R_r L_s \end{bmatrix} \quad (6)$$

$$A_3 = \begin{bmatrix} L_r & 0 & -L_m & 0 \\ 0 & L_r & 0 & -L_m \\ -L_m & 0 & L_s & 0 \\ 0 & -L_m & 0 & L_s \end{bmatrix} \quad (7)$$

where, V_{ds} and V_{qs} are $d-$ and $q-axis$ stator voltages, V_{dr} and V_{qr} are $d-$ and $q-axis$ rotor voltages, I_{ds} and I_{qs} are $d-$ and $q-axis$ stator currents, I_{dr} and I_{qr} are $d-$ and $q-axis$ rotor currents, Φ_{ds} and Φ_{qs} are $d-$ and $q-axis$ stator fluxes, Φ_{dr} and Φ_{qr} are $d-$ and $q-axis$ rotor fluxes, P_s and Q_s are stator active and reactive powers, R_s and R_r are stator and rotor resistances, L_s, L_r and L_m are stator, rotor and magnetizing inductance, $\sigma = 1 - \frac{L_m^2}{L_s L_r}$ is the dispersion coefficient, ω_s is the rotating frame speed, ω_m is the rotor speed, p is the number of machine pole pairs.

III. STATOR FIELD ORIENTATION

The field-oriented control is consisting of orienting the stator or rotor flux axis along the $d-axis$ which allows achieving a decoupling between the $d-$ and $q-axis$ so that the control of DFIG active and reactive powers can be independent[31,32]. For the DFIG, the orientation of the stator flux is achieved as follows:

$$\Phi_{qs} = 0 \Longrightarrow \Phi_{ds} = \Phi_s \quad (8)$$

According to the flux orientation given by Eqs. (8), the DFIG voltages and currents become:

$$I_{ds} = \Phi_s - \frac{L_m}{L_s} I_{dr} \quad (9a)$$

$$I_{qs} = -\frac{L_m}{L_s} I_{qr} \quad (9b)$$

$$V_{ds} = 0 \quad (10a)$$

$$V_{qs} = V_s = R_s I_{qs} + \omega_s \Phi_{ds} \quad (10b)$$

$$V_{dr} = R_r I_{dr} + \frac{d\Phi_{dr}}{dt} - \omega_s \Phi_{qr} \quad (10c)$$

$$V_{qr} = R_r I_{qr} + \frac{d\Phi_{qr}}{dt} + \omega_s \Phi_{dr} \quad (10d)$$

with V_s and Φ_s are stator voltage and flux resulting from the field orientation condition. By using equations 9 and 10, the stator powers and the electromagnetic torque become:

$$P_s = -(V_s \frac{L_m}{L_s}) I_{qr} \quad (11a)$$

$$Q_s = \frac{V_s^2 \Phi_s}{L_s} - (V_s \frac{L_m}{L_s}) I_{dr} \quad (11b)$$

$$T_e m = -\frac{pL_m}{L_s}) I_{qr} \Phi_s \quad (11c)$$

By combining Eqs. (4), Eqs. (9) and Eqs. (10), the rotor voltage equations become:

$$V_{dr} = R_r I_{dr} + (L_r - \frac{L_m^2}{L_s}) \frac{dI_{dr}}{dt} - e_d \quad (12a)$$

$$V_{qr} = R_r + (L_r - \frac{L_m^2}{L_s}) \frac{dI_{qr}}{dt} + e_q \quad (12b)$$

With e_d and e_q are the coupling part given by:

$$e_d = s\omega_s (L_r - \frac{L_m^2}{L_s}) I_{qr} \quad (13a)$$

$$e_q = s\omega_s (L_r - \frac{L_m^2}{L_s}) I_{dr} + s\frac{L_m V_s}{L_s} \quad (13b)$$

with $s = 1 - \frac{\omega_m}{\omega_s}$ is the machine slip

IV. FUZZY LOGIC-BASED NEURAL NETWORK CONTROL

The neural network is a mathematical model that imitates the operating mode of human nervous system. The feedforward multilayer structure is mostly used, where the neural network is created by a set of artificial neurons weightily connected organised in a number of layers and equipped with an activation functions to perform a well-defined task. Considered as an universal approximator, the multilayer neural network allows the approximation of divers non-linear behaviour from an input-output data set and a training phase.

The used NNCs are designed and trained from a control scheme involving the orientation of the DFIG stator field associated with FLC. Using equations 13, two FLC are selected for the control of the DFIG active and reactive powers as illustrated on Fig. 2. The FLC scheme is then exploited to provide the inputs-outputs set needed for the NNC training process. The rotor currents errors and current error variations are used as inputs for the NNs controllers while the rotor voltages are used as outputs.

ACCEPTED MANUSCRIPT
Journal of Renewable and Sustainable Energy
AIP Publishing
This is the author's peer reviewed, accepted manuscript. However, the online version of record will be different from this version once it has been copyedited and typeset.
PLEASE CITE THIS ARTICLE AS DOI: 10.1063/5.0125713

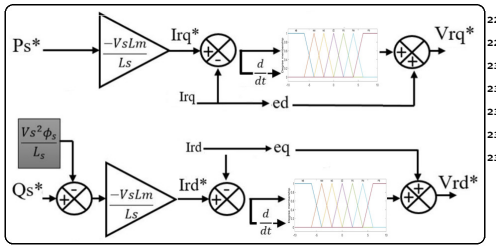


FIG. 2. FLC-based field oriented control for DFIG rotor currents.

In figure 2, P_s^* and Q_s^* are stator active and reactive powers, I_{rq}^* and I_{rd}^* are stator current references resulting from powers references and V_{rq}^* and V_{rd}^* are stator control voltages resulting from control.

After a training phase, the resulting NNCs are used in the control scheme instead of fuzzy logic controllers as shown on Fig. 3 for the active and reactive powers control. The substitution of fuzzy logic controllers by NNCs ones is motivated by two reasons. Firstly and, with the same performances and robustness features the NNCs are more simpler for designing and implementation ([33–36]). Secondly, the NNCs are better suited for the approach that will be proposed later for more simplification of the DFIG control scheme.

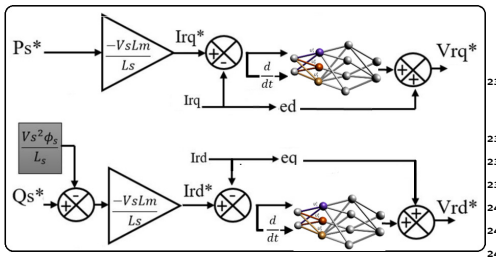


FIG. 3. NN control diagram for DFIG rotor currents

V. THE M5P-DTA-BASED CONTROL

The M5P-DTA is one of the faster machine learning algorithms. This algorithm is based on a combination between the decision tree algorithm and the linear regression algorithm. Generally, the obtained tree model is composed of three nodes called: root node, internal node, and leaf node. These nodes are interconnected with branches as illustrated in Fig. 4. In the present section, this algorithm is proposed to enhance the neural network controller, specially in processing time. The used M5P-DTA is based on standard deviation (SD) as splitting criteria, that is mean that the attribute that has the maximum SD is the selected one. In this later a linear model is used for leaves of regression trees to predict the values of the numeric response variable. i.e. the last nodes are linear regression functions that can give continuous numeric attributes as in Figure 5. The algorithm works by dealing with the standard deviation of the class values in a node as error measurement and calculates the expected reduction of this error as a result of the test of each attribute and the target in this node. The M5P model works in many stages[37].

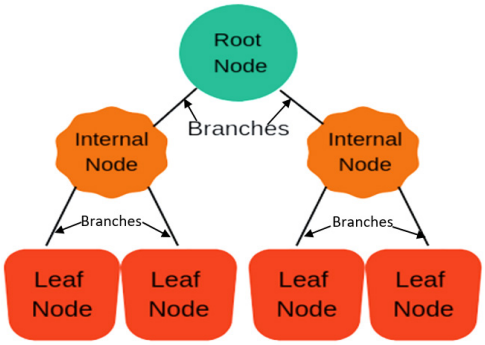


FIG. 4. Basic diagram of the M5P algorithm.

A. Decision tree

In this first stage, a nominal output based on a data set is provided from a class label predicted by a form of construction tree and generalized as a non-parametric model during the training phase, thus allowing the correct classification of unseen data in most of the cases. The growth phase is based on the values of the attributes to subdivide the nodes. The model composes of three different nodes called, the roots node contains the attribute that has the maximum standard deviation reduction, the internal node, and the terminal node (leaf). The main objective is to increase the depth of the tree by the reduction of the data-set to a smaller subset, then the multiple regression model is constructed. Based on minimizing the prediction errors of the numerical responses, an attribute is chosen and used to split the data set at each node. The prediction error is calculated by measuring the standard deviation reduction (SDR) which is expressed by[38,39]:

$$SDR = SD(T) - \Sigma_i \frac{T_i}{|T|} SD(T) \tag{14}$$

Where T is the input data set that reaches the node, T_i is the resulting sets of the split node via the chosen attribute and the SD represents the standard deviation.

ACCEPTED MANUSCRIPT
Journal of Renewable and Sustainable Energy
AIP Publishing
This is the author's peer reviewed, accepted manuscript. However, the online version of record will be different from this version once it has been copyedited and typeset.
PLEASE CITE THIS ARTICLE AS DOI: 10.1063/5.0125713

B. The linear regression

The linear regression is a statistical tool used to establish forecasts whose purpose is to estimate the relationship between two or more variables to develop a linear function. Talking about simple regression when we have an independent variable or multiple regression when we have several explanatory variables as used in the M5P-DTA which represents an advantage due to its efficient and simple model. Based on the set of examples reaching the node, a multi-linear regression model is built for each leaf, Fig. 5. A simplification of the regression model is realized for the case of predicted error diminution for the future data. Equation 15 expresses the general form of the linear model (*LM*). The minimization of the least squares error of the actual and predicted values of the training data (Eq. 16) and performed by the algorithm allowing the weight of the linear model to be calculated[40].

$$LM_j = \omega_{j0} + \omega_{j1}a_1 + \cdots + \omega_{jk}a_k \tag{15}$$

$$Min\Sigma(T - T')^2 \tag{16}$$

With LM_j is the linear model number j, ω_{ji} are the weights of the linear model LM_j and a_i are the attribute value.

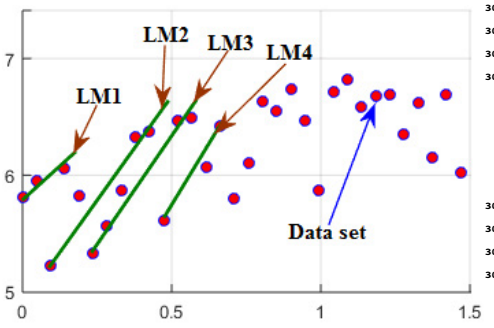


FIG. 5. Multi-linear regression for the data set.

C. Pruning step

The current phase is so important that it allows the model to be improved. Usually, the M5P algorithm provides a complicated initial model, this latter may have unnecessary sub-trees, nodes and branches, which may lead to a wrong prediction for the invisible set. The pruning phase consists in deleting these branches or sub-trees to have a tree model of minimal size and more efficient prediction accuracy. At each instant when the reduction of the estimated error is performed, the tree is pruned. The estimation process of the mean absolute error (MAE) between the actual value T and the predicted value T' (Eqs. (17)) reaching the present node allows the compensation between the tree unpruned and pruned models ([37–41]).

$$MAE = \frac{1}{N}\Sigma_i^N \mid T - T' \mid \tag{17}$$

Where N represents the number of examples. The mean absolute error estimation of the samples reaching the current node generally underestimates the predicted error of the unseen cases, a compensation via multiplication by a factor is carried out, to minimize the estimated error.

$$\frac{n+v}{n-v} \tag{18}$$

While n represents the number of learning instances reaching the node and v is the number of elements in the model representing the value at that node[38].

D. The smoothing process

In this step and behind, the model is improved from an accuracy point of view through the smoothing process. For a pruned tree model, the discontinuity model is unavoidable for linear models adjacent to the leaf level. The step is important precisely for the models obtained with a low number of training and thus which contain different scenarios. the smoothing is expressed by p' and calculated as follows[38,41] :

$$p' = \frac{n_p + k_p}{n + k} \tag{19}$$

Where p is the predicted value given to the current node, q is the model predicted value in the current node, n is the number of training examples, and k is a constant which equals to 15.

E. Training phase

The aim of this paper is to project a new artificial intelligence algorithm to bring improvements to the indirect control of the active and reactive stator powers of DFIG. The experience takes place by synthesizing an algorithm defined by a simple If-Then script which makes it possible to replace the neural network controllers. The M5P model is schematized based on the inputs and outputs of the data set collected from the NNC test. The data set of 10000 test instances of inputs and outputs are characterized by error, error variation of rotor currents I_{dr}, I_{qr}, and rotor voltage reference targets are used to synthesize a script of 20 rules for active power and 42 rules for reactive power. Indeed, 66% of the data is used for training and the rest is used for testing, Fig. 6. The decision tree model is obtained using weka software based on the NNC test data-set.

ACCEPTED MANUSCRIPT
Journal of Renewable and Sustainable Energy
AIP Publishing
This is the author's peer reviewed, accepted manuscript. However, the online version of record will be different from this version once it has been copyedited and typeset.
PLEASE CITE THIS ARTICLE AS DOI: 10.1063/5.0125713

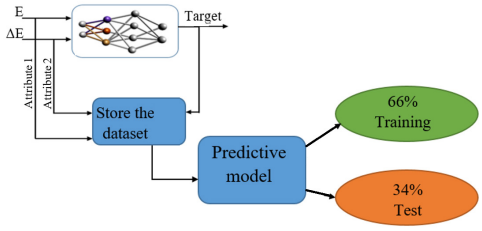


FIG. 6. data-set distribution for training and testing process.

In this study, the generated active and reactive power control is carried out through the rotor current control. The proposed algorithm replaces the neural network controllers as it is described in Fig. 9. Tree models are obtained for $d-$ and $q-$axes via the learning process by using the collected examples of errors, errors variation, and rotor voltage references introduced in WEKA software.

After the different process steps mentioned previously, Fig. 7 and 8 show the M5 pruned tree model, the script rules and the decision tree for quadratic (I_{rq}) and direct rotor currents (I_{rd}). The active power control containing 20 rules while the reactive power control is achieved with 42 rules. Table I represents the obtained test results for both I_{rq} and I_{rd}.

TABLE I. Rotor currents tests results..

	I_{qr}	I_{dr}
Time taken to build model	0.65s	0.65s
Time taken to test model on test split	0.04	0.04
Correlation coefficient	0.9999	0.9999
Mean absolute error	0.0004	0.0004
Root mean squared error	0.0012	0.0012
Relative absolute error	0.9392	0.9392
Root relative squared error	1.491	1.491
Total Number of Instances	3400	3400

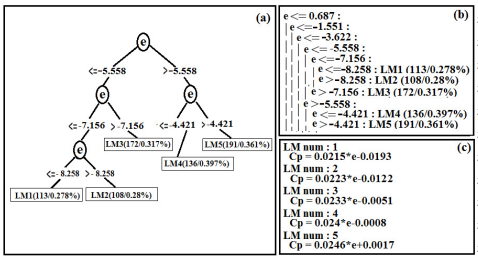


FIG. 7. M5P algorithm for I_{rq} : (a) The target attribute weights, (b) The script rules, (c) The decision tree .

Fig. 9 illustrates the proposed M5P tree model control scheme. The I_{rd} control is done via decision rule using error and error variation while the I_{rq} control required only the error parameter.

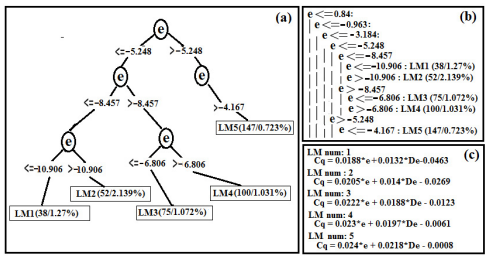


FIG. 8. M5P algorithm for I_{rd} : (a) The target attribute weights, (b) The script rules, (c) The decision tree .

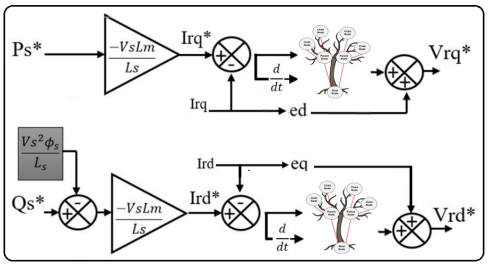


FIG. 9. M5P algorithm control diagram for DFIG rotor currents.

VI. DATA MANAGEMENT

To realize the decision tree model, a data-set is needed to establish the training process. Indeed, the tree model is proposed whose main purpose is to improve the control scheme of the rotor currents I_{rq} and I_{rd}, to better control the stator's active and reactive powers. An experimental test based on the NNC was carried out and recorded via the Control-Desk software for 30s. Through this recording, an input/output data set of appropriate size has been collected for the NNC training process. The control scheme uses two NNCs, one for active power and the other for reactive power. the first NNC has as inputs the error and error variations of quadratic current I_{rq} (Fig. 10-a and 10-b) and as output the quadratic rotor voltage V_{rq} (10-c). For the second NNC, the input are the error and error variations of direct current I_{rd} (Fig. 11-a and 11-a) and the output is the direct rotor voltage V_{rd} (Fig. 11-c).

After the NNCs training process, the WEKA software and from the trained NNCs parameters generates the wanted decision tree model that is a simple set of 'IF-THEN' rules. Finally, the resulting tree model is inserted in the control bloc to substitute the two NNCs, Fig. 9. During implementation phase, some inputs/outputs set is recorded and used to check the established tree-model. Fig. 10-c and Fig. 11-c show that

ACCEPTED MANUSCRIPT
Journal of Renewable and Sustainable Energy
AIP Publishing
This is the author's peer reviewed, accepted manuscript. However, the online version of record will be different from this version once it has been copyedited and typeset.
PLEASE CITE THIS ARTICLE AS DOI: 10.1063/5.0125713

the output voltage for both NNCs and tree models are very closes.

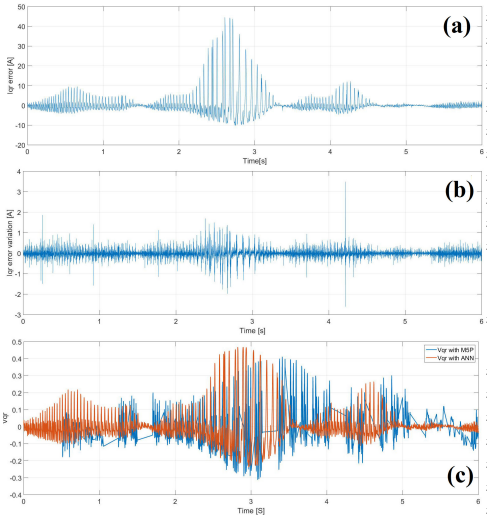


FIG. 10. Training data for active power control : (a) I_{qr} error, I_{qr} error variation, (c) Quadratic rotor voltage V_{qr}

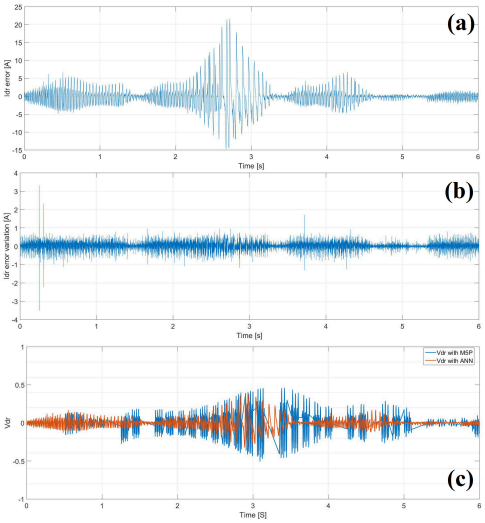


FIG. 11. Training data for reactive power control : (a) I_{dr} error, I_{dr} error variation, (c) Quadratic rotor voltage V_{dr} .

VII. RESULTS AND DISCUSSIONS

In this paper, a comparative study is performed and applied to the 1.5 kW WECS representing a DFIG driven by a wind emulator based on a DC motor. The study permits the indirect control of the DFIG stator active and reactive powers through rotor currents I_{rq} and I_{rd}. Firstly, an NNC is built and applied to the rotor currents control. Then to improve the control results, the decision tree algorithm is built to replace the NN controllers. In addition, a PI-based control scheme is performed for a comparison purpose.The work carried out involves both simulation tests and an experimental tests. The parameters of the used DFIG are: $R_s = 4.85\Omega$, $R_r = 3.805\Omega$, $L_s = L_r = 0.274H$, $L_m = 0.258H$.

A. Simulation results

The simulation test is carried out for 30s at variable speed by using the real parameters of the DFIG which is used in the experiment study step.

Fig. 12 shows the active power control result by using standard PI, the NNC and the M5P-DTA. The active power reference is imposed from the MPPT strategy, we can notice that the emulator based on the DC motor is driven to provide an active power profile close to that of a real wind model. During the test, The reference power is varying between 0 and 1500 watts. The control has been performed with good tracking of the reference power for the three controls, except that the result obtained by applying the M5P-DTA is better than that obtained with the NNC and the conventional PI where the chattering is significantly reduced.

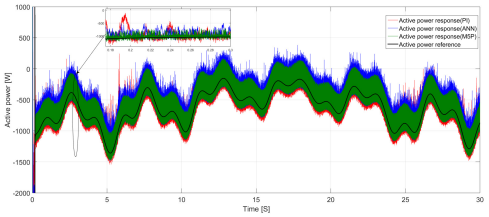


FIG. 12. Stator active power.

The result of the reactive power control is illustrated in Fig. 13, a constant reference value was imposed from outside equal to 763 Var to keep the direct current I_rd equal to zero during the test. It is noticed that the measured variables track perfectly the references with an improvement by applying the M5P-DTA.

Fig. 14 and 15 represent the rotor currents evolution. It is obvious that the currents I_rd and I_rq are respectively the images of the reactive and active powers and take the same shape as theses powers, see equations 12. For both currents the control is performed with a good dynamic performance with more reduction of the chattering phenomenon on the side

ACCEPTED MANUSCRIPT
Journal of Renewable and Sustainable Energy
AIP Publishing
This is the author's peer reviewed, accepted manuscript. However, the online version of record will be different from this version once it has been copyedited and typeset.
PLEASE CITE THIS ARTICLE AS DOI: 10.1063/5.0125713

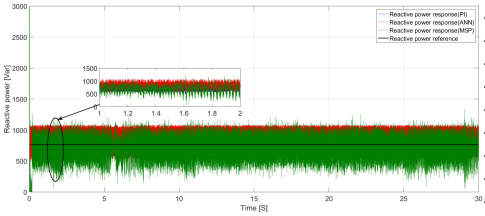


FIG. 13. Stator reactive power.

of the M5P-DTA compared to the other controls.

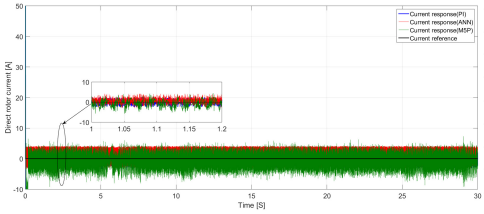


FIG. 14. Direct rotor current.

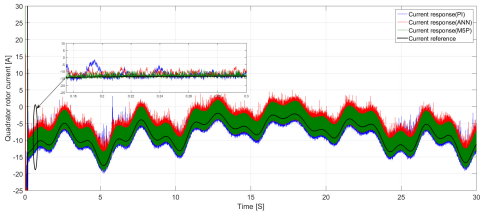


FIG. 15. Quadratic rotor current.

B. Experimental results

Fig. 16 describes the workbench which allows realizing the experimental test of the WECS. The test and its results have been done through MATLAB/SIMULINK software, the dSPACE DS1104 control board, and the Control-Desk graphical interface.

The first part consists in implementing the wind emulator based on a Dc motor. By choosing an appropriate wind profile, the Dc motor speed is controlled so that this last generate the reference values for the DFIG active power, given in Fig. 17. The results of active power obtained with the conventional PI controller (Fig. 17-a), the NNC (Fig. 17-b) and the M5P-DTA (Fig. 17-c). As in simulation, the control is performed correctly in experimental test, with a more improved tracking is seen in the M5P-DTA results. Indeed, the M5P-DTA makes it possible to eliminate the important oscillations appearing in the classic PI results, when the power exceeds 500W as well as to reduce the delay, between the active power and its reference, seen in the NNC results.

The reactive power is represented by Fig. 18, it remains at a constant value of 763Var throughout the test, which means that there is no reactive power transaction between the DFIG stator side and the grid, since the direct current i_{dr} is equal to zero (Fig. 20). Moreover, important peaks reaching 1200 Var are noticed in the PI results (Fig. 18-a), they are reduced by the NNC to around 950 Var (Fig. 18-b) and they not exceed 900 Var for the M5P-DTA model (Fig. 18-c).

Fig. 19 and Fig. 20 show respectively the quadratic and direct currents (i_{qr}, i_{dr}). Similar to active and reactive powers results, the use of the PI makes important oscillations and peaks appear that are reduced by NNC and M5P-DTA controllers. A precision improvement is seen with the M5P-DTA (Fig. 19-c) which corrects the NNC tracking delay (Fig. 19-b).

Fig. 21 and Fig. 22 respectively represent the active power, the reactive powers and the rotor currents. the graphs describe the results obtained previously and recorded by the oscilloscope for both NNC and M5P-DTA.

Across the experiment results, we addict that, even if the PI controller is easy to implement, its use generates large oscillations and important peaks in powers and currents during the test, which can be dangerous for the machine. Applying the neural network controllers reduced these problems, but the NNC-based M5P-DTA allows enhancing more the control and obtain better results. Another interesting feature of the algorithm is that compared to other techniques such as PI controller[2,5,6], neural networks[22,23], fuzzy logic[19,21], sliding mode[8,11], backstepping[16] and other techniques[29,42–44], it gives the same even better performances (for some cases) with a very reduced processing time.

DATA AVAILABILITY STATEMENT

The data that support the findings of this study are available from the corresponding author upon reasonable request.

VIII. CONCLUSION

In this paper, an experimental study of the wind energy conversion system is carried out to obtain an improvement of the indirect control of stator active and reactive powers of the doubly fed induction generator. A wind emulator based on a DC motor is realized to generate the active power reference values used for the experimental test. The stator powers are controlled indirectly via the rotor currents. At first, two NNCs were trained based on well-designed fuzzy logic controllers and then inserted into the DFIG control scheme. Subsequently, an M5P decision tree algorithm is applied for the optimization of the obtained NNCs. Also and, for a comparison purpose, a control scheme based on a standard PI was performed. The obtained results , whether experimental or by

AIP Publishing
Journal of Renewable and Sustainable Energy
ACCEPTED MANUSCRIPT
This is the author's peer reviewed, accepted manuscript. However, the online version of record will be different from this version once it has been copyedited and typeset.
PLEASE CITE THIS ARTICLE AS DOI: 10.1063/5.0125713

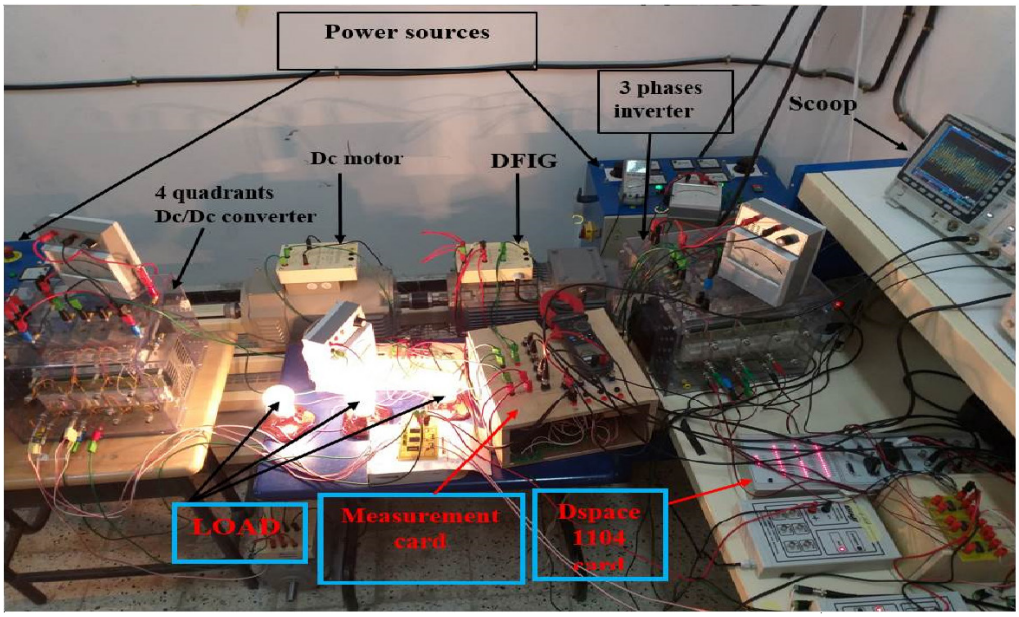


FIG. 16. Experimental bench.

simulation, show that the proposed controller has improved the control of the DFIG from different sides. On the performance side, the M5P-DTA has made it possible to eliminate the oscillations and perturbations caused by the PI regulator, in particular for high powers, as well as to reduce the peaks in powers and currents which become less, even compared to the NNC. On the processing time side, the configuration and operating mode of the M5P-DTA allow it to complete the control task in a faster way compared to NNC, fuzzy logic controllers and even to standard PI. This feature is very appreciated during the implementation of complicated control systems such as that corresponding to the DFIG where a fast calculation time makes it possible to expand the control aims without requiring more sophisticated processing tools.

[1]H. F. Rashag, S. P. Koh, A. N. Abdalla, N. M. L. Tan, and K. H. Chong, Journal of Power Electronics **13**, 369 (2011).
[2]A. Zemmit, S. Messalti, and A. Harrag, Ain Shams Engineering Journal **9**, 1877 (2018).
[3]F. M. Gebru, B. Khan, and H. H. Alhelou, Comput. Electr. Eng. **86**, 106727 (2020).
[4]A. Djoudi, S. Bacha, and H. Iman-Eini, Journal of Renewable and Sustainable Energy **11**, 025503 (2019).
[5]A. Tamaarat and A. Benakcha, Front. Energy. **8**, 371 (2014).
[6]Y. Djeriri, A. Meroufel, A. Massoum, and Z. Boudjema, Journal of Electrical Engineering. **14**, 169 (2014).
[7]M. Verij Kazemi, S. A. Gholamian, and J. Sadati, Journal of renewable and sustainable energy **11**, 043305 (2019).
[8]E. G. Shehata, Alexandria Engineering Journal. **54**, 1067-1075 (2015).
[9]Y. Zhang, J. Jiao, and D. Xu, IEEE Trans. Power Electron. **34**, 12024-12037 (2019).
[10]S. V. Savarkar, G. Dyanamina, and S. B. Singh, in *Proceedings of the International Conference on Advances in Electronics, Electrical and Computational Intelligence (ICAEEC)* (SSRNs eLibrary, Allahabad, India, 2019).
[11]X. Zhu, S. Liu, and Y. Wang, in *Proceedings of the 3rd Renewable Power Generation Conference* (Naples, Italy, 2014).
[12]S. Ebrahimkhani, ISA Trans. **63**, 343 (2016).
[13]M. Fdaili, A. Essadki, and T. Nasser, Int. J. Renew. Energy Res. IJRER. **7**, 2151 (2017).
[14]M. J. Morshed and A. Fekih, in *Proceedings of 2017 American Control Conference (ACC)* (ACC, Seattle, WA, USA, 2017) pp. 729–734.
[15]H. Delavari and A. Sharifi, Journal of Renewable and Sustainable Energy **13**, 033311 (2021).
[16]M. Nadour, A. Essadki, and T. Nasser, Int. J. Renew. Energy Res. **7**, 1307 (2017).
[17]R. Sadeghi, S. M. Madani, M. Ataei, M. R. A. Kashkooli, and S. Ademi, IEEE Trans. Ind. Electron. **65**, 9147 (2018).
[18]H. Benbouhenni, Z. Boudjema, and A. Belaidi, Journal Europ; des Syst. Autom. **53**, 69 (2020).
[19]M. M. Ismail and A. F. Bendary, Alexandria Engineering Journal. **55**, 941 (2016).
[20]A. Benyamina, S. Moulahoum, I. Colak, and R. Bayindir, Electr. Power Syst. Res. **152**, 357 (2017).
[21]B. P. Ganthia and S. K. Barik, J. of The Institution of Engineers (India): Series B. **101**, 273 (2020).
[22]M. Hallouz, N. Kabache, S. Moulahoum, and S. Kouadria, Int. J. Smart Grid-IjSmartGrid. **2**, 183-187 (2018).
[23]M. R. Douiri, A. Essadki, and M. Cherkaoui, Procedia Comput. Sci. **127**, 454 (2018).
[24]T. H. Chien, Y. C. Huang, and Y. Y. Hsu, Energies. **13**, 5320 (2020).
[25]I. K. Amin, M. N. Uddin, and M. Marsadek, in *Proceedings of 2019 IEEE International Electric Machines and Drives Conference (IEMDC)* (San Diego, CA, USA, 2019) p. 2077-2082.

ACCEPTED MANUSCRIPT
Journal of Renewable and Sustainable Energy
AIP Publishing
This is the author's peer reviewed, accepted manuscript. However, the online version of record will be different from this version once it has been copyedited and typeset.
PLEASE CITE THIS ARTICLE AS DOI: 10.1063/5.0125713

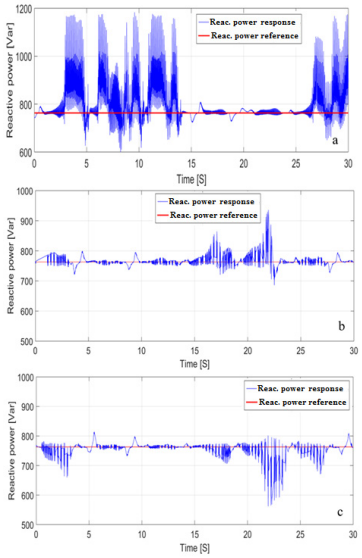


FIG. 17. Active power responses: (a). PI controller, (b) NNC, (c). M5P-DTA.

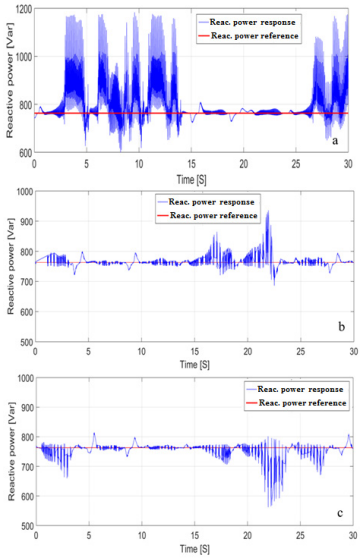


FIG. 18. Reactive power responses: (a). PI controller, (b) NNC, (c). M5P-DTA.

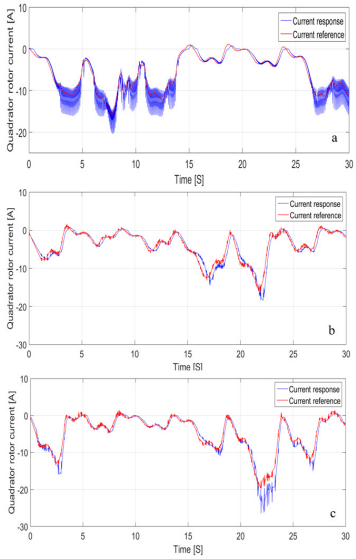


FIG. 19. Quadratic rotor current: (a). PI controller, (b) NNC, (c). M5P-DTA.

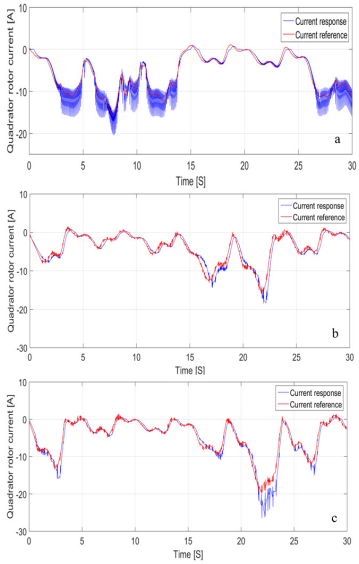


FIG. 20. Direct rotor current: (a). PI controller, (b) NNC, (c). M5P-DTA.

ACCEPTED MANUSCRIPT
Journal of Renewable and Sustainable Energy
AIP Publishing
This is the author's peer reviewed, accepted manuscript. However, the online version of record will be different from this version once it has been copyedited and typeset.
PLEASE CITE THIS ARTICLE AS DOI: 10.1063/5.0125713

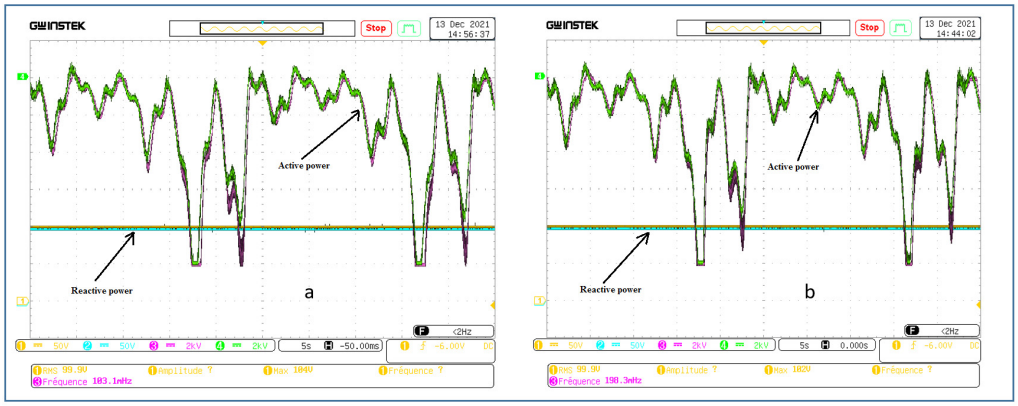


FIG. 21. Active and reactive power: (a) NNC, (b) M5P-DTA.

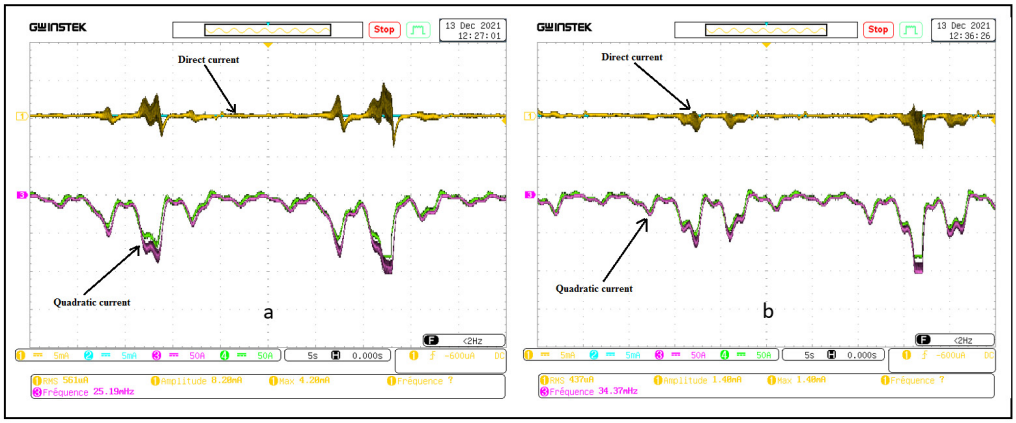


FIG. 22. Rotor currents I_{dr} I_{qr}: : (a) NNC, (b) M5P-DTA.

[26]K. H. Kim, T. L. Van, D. C. Lee, S.-H. Song, and E.-H. Kim, IEEE Trans. Ind. Electron. **60**, 3207 (2012).
[27]A. G. Abo-Khalil, A. S. Alghamdi, A. M. Eltamaly, M. S. Al-Saud, K. Sayed, G. R. Bindu, and I. Tlili, IEEE Trans. Ind. Electron. **12**, 2427 (2019).
[28]K. K. Jaladi, K. S. Sandhu, and P. Bommala, J. Control Autom. Electr. Syst. **31**, 402 (2020).
[29]M. A. Soomro, Z. A. Memon, M. Kumar, and M. H. Baloch, Energy Reports. **7**, 6031-6043 (2021).
[30]S. Kouadria, E. M. Berkouk, Y. Messlem, and M. Denaï, Journal of Renewable and Sustainable Energy **10**, 043306 (2018).
[31]B. Rached, M. Elharoussi, and E. Abdelmounim, in *Proceedings of 2019 International Conference of Computer Science and Renewable Energies (ICCSRE)* (IEEE, Agadir, Morocco, 2019) pp. 1–-6.
[32]E. Elbouchikhi, G. Feld, Y. Amirat, M. Benbouzid, and F. L. Gall, Comput. Electr. Eng. **84**, 106661 (2020).
[33]M. Mujammal, A. Moualdia, and D. Boudana, in *Proceedings of 18th International Multi-Conference on Systems, Signals Devices (SSD)* (Tunisia, 2021) pp. 563–568.
[34]D. E. Beladjine, D. Boudana, A. Moualdia, M. Hallouz, and P. Wira, in *Proceedings of 18th International Multi-Conference on Systems, Signals Devices (SSD)* (Tunisia, 2021) pp. 1291–1295.
[35]N. Kabache and S. Moulahoum, in *Proceedings of 4Th International Conference on electrical engineering* (Algiers, Algeria, 2012) pp. 449–454.
[36]A. Xu, H. Chang, Y. Xu, R. Li, X. Li, and Y. Zhao, Waste Manag. **124**, 385 (2021).
[37]R. Benkercha and S. Moulahoum, Sol. Energy. **173**, 610 (2018).
[38]S. Blaifi, S. Moulahoum, R. Benkercha, B. Taghezouit, and A. Saim, Sol. Energy. **163**, 405-424 (2018).
[39]A. Etemad-Shahidi and J. Mahjoobi, Ocean Eng. **163**, 1175 (2009).
[40]J. Zahiri and H. Nezaratian, Environ. Sci. Pollut. Res. **27**, 14553 (2020).
[41]J. R. Quinlan, in *Proceedings of Australian Joint Conference on Artificial Intelligence*, edited by Adams and Sterling (, Hobart, Australia, 1992) pp. 343–348.
[42]F. Poitiers, T. Bouaouiche, and M. Machmoum, Electric Power Systems Research **79**, 1085 (2009).

AIP Publishing
Journal of Renewable and Sustainable Energy
ACCEPTED MANUSCRIPT
This is the author's peer reviewed, accepted manuscript. However, the online version of record will be different from this version once it has been copyedited and typeset.
PLEASE CITE THIS ARTICLE AS DOI: 10.1063/5.0125713

[43]N. E. Karakasis and C. A. Mademlis, Renewable Energy **125**, 974 (2018). [44]A. Kasbi and A. Rahali, Materials Today: Proceedings **45**, 5426 (2021).

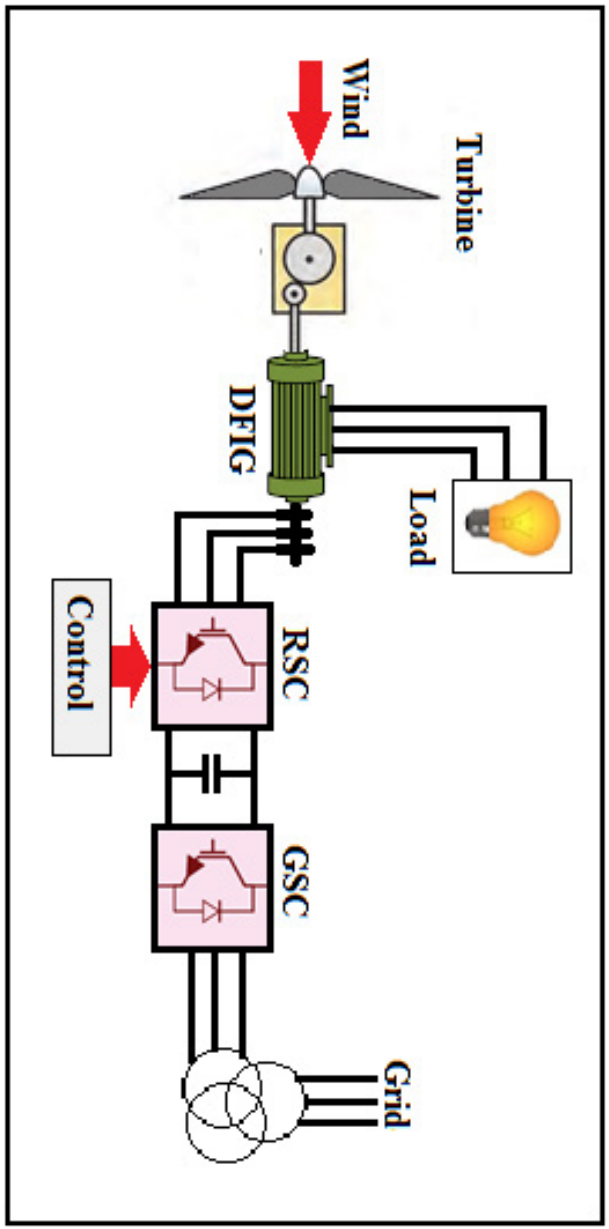
AIP Publishing

Journal of Renewable and Sustainable Energy

ACCEPTED MANUSCRIPT

This is the author's peer reviewed, accepted manuscript. However, the online version of record will be different from this version once it has been copyedited and typeset.

PLEASE CITE THIS ARTICLE AS DOI: 10.1063/5.0125713



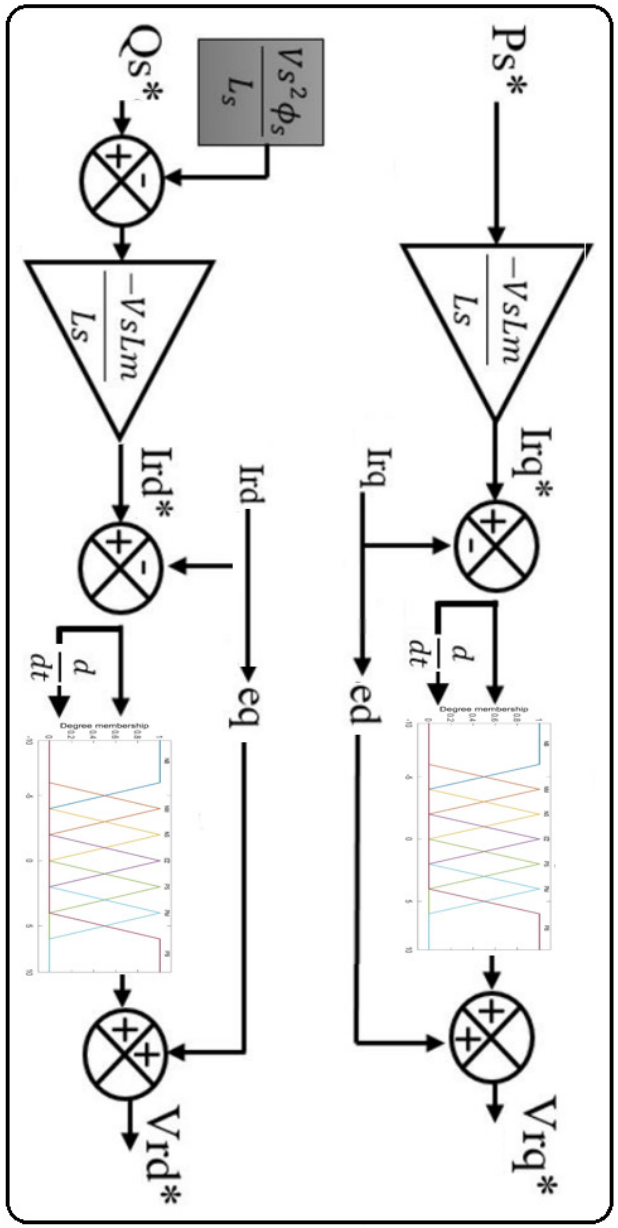
AIP Publishing

Journal of Renewable and Sustainable Energy

ACCEPTED MANUSCRIPT

This is the author's peer reviewed, accepted manuscript. However, the online version of record will be different from this version once it has been copyedited and typeset.

PLEASE CITE THIS ARTICLE AS DOI: 10.1063/5.0125713



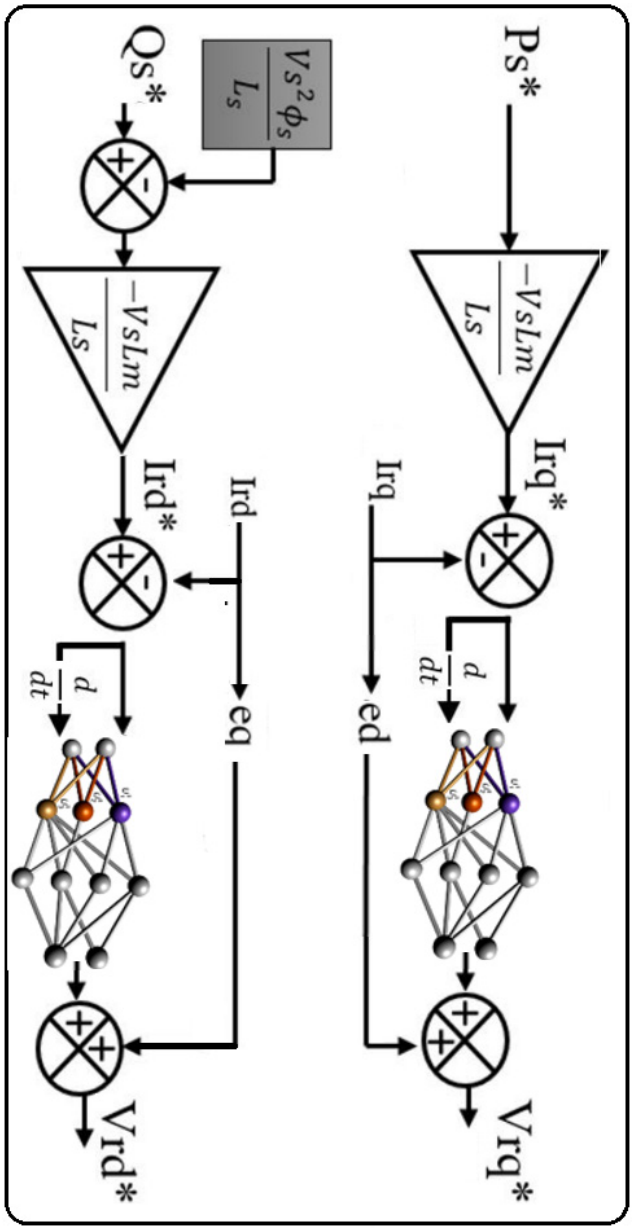
AIP Publishing

Journal of Renewable and Sustainable Energy

ACCEPTED MANUSCRIPT

This is the author's peer reviewed, accepted manuscript. However, the online version of record will be different from this version once it has been copyedited and typeset.

PLEASE CITE THIS ARTICLE AS DOI: 10.1063/5.0125713



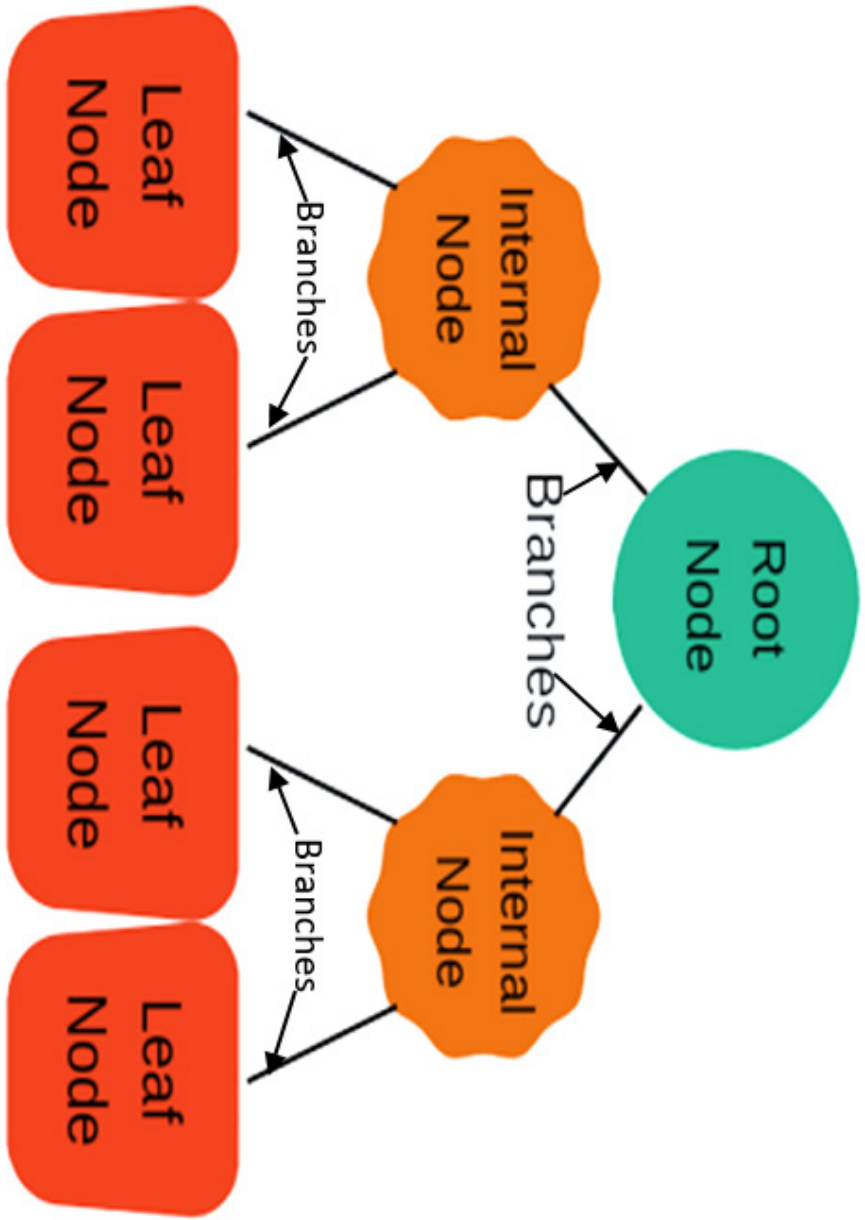
AIP Publishing

Journal of Renewable and Sustainable Energy

ACCEPTED MANUSCRIPT

This is the author's peer reviewed, accepted manuscript. However, the online version of record will be different from this version once it has been copyedited and typeset.

PLEASE CITE THIS ARTICLE AS DOI: 10.1063/5.0125713



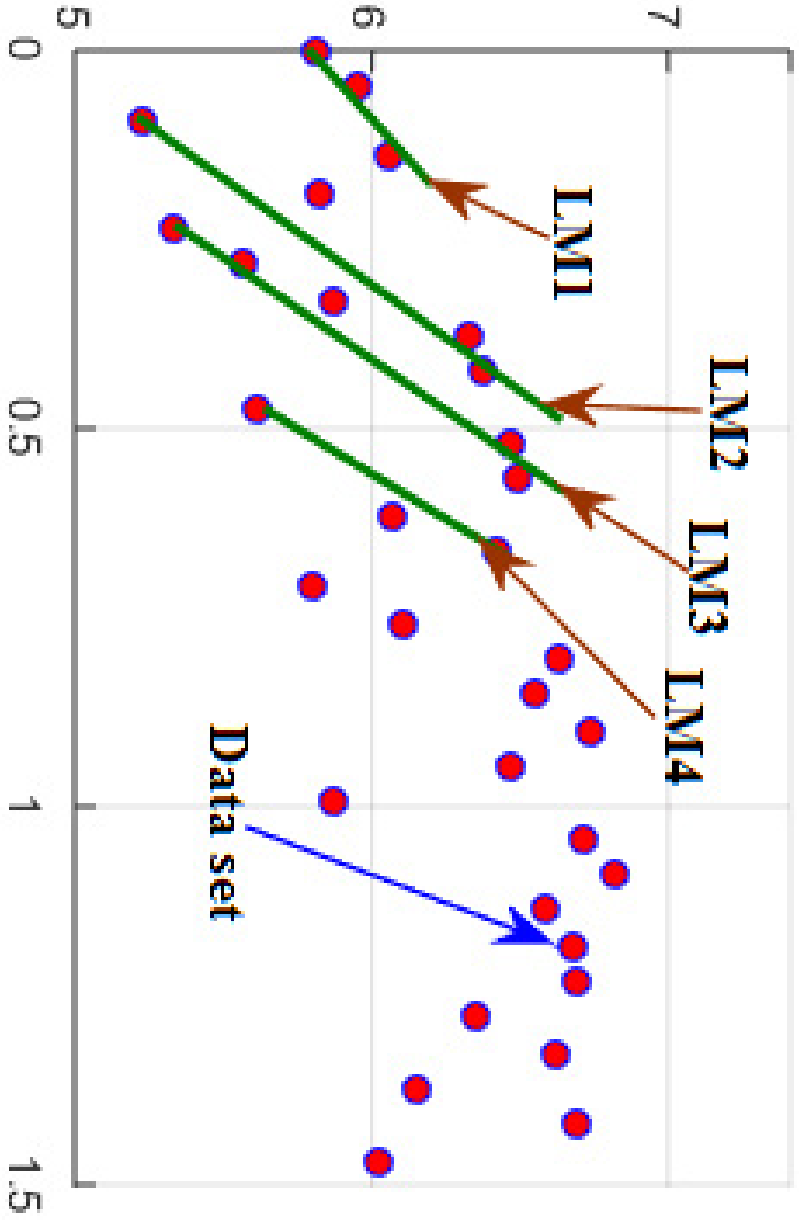
AIP Publishing

Journal of Renewable and Sustainable Energy

ACCEPTED MANUSCRIPT

This is the author's peer reviewed, accepted manuscript. However, the online version of record will be different from this version once it has been copyedited and typeset.

PLEASE CITE THIS ARTICLE AS DOI: 10.1063/5.0125713



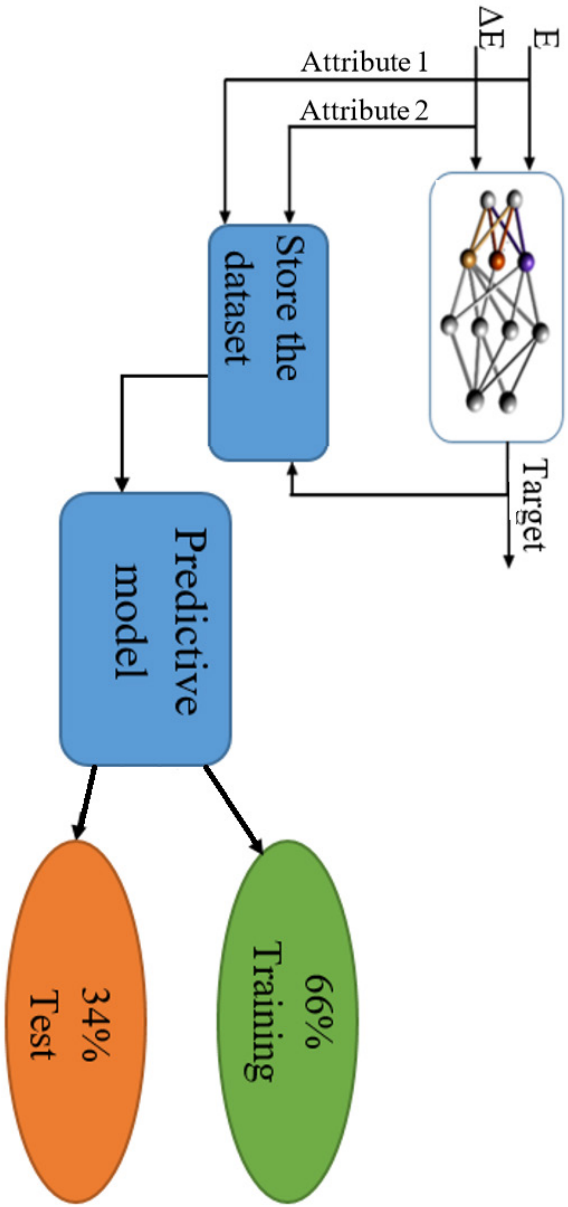
AIP Publishing

Journal of Renewable and Sustainable Energy

ACCEPTED MANUSCRIPT

This is the author's peer reviewed, accepted manuscript. However, the online version of record will be different from this version once it has been copyedited and typeset.

PLEASE CITE THIS ARTICLE AS DOI: 10.1063/5.0125713



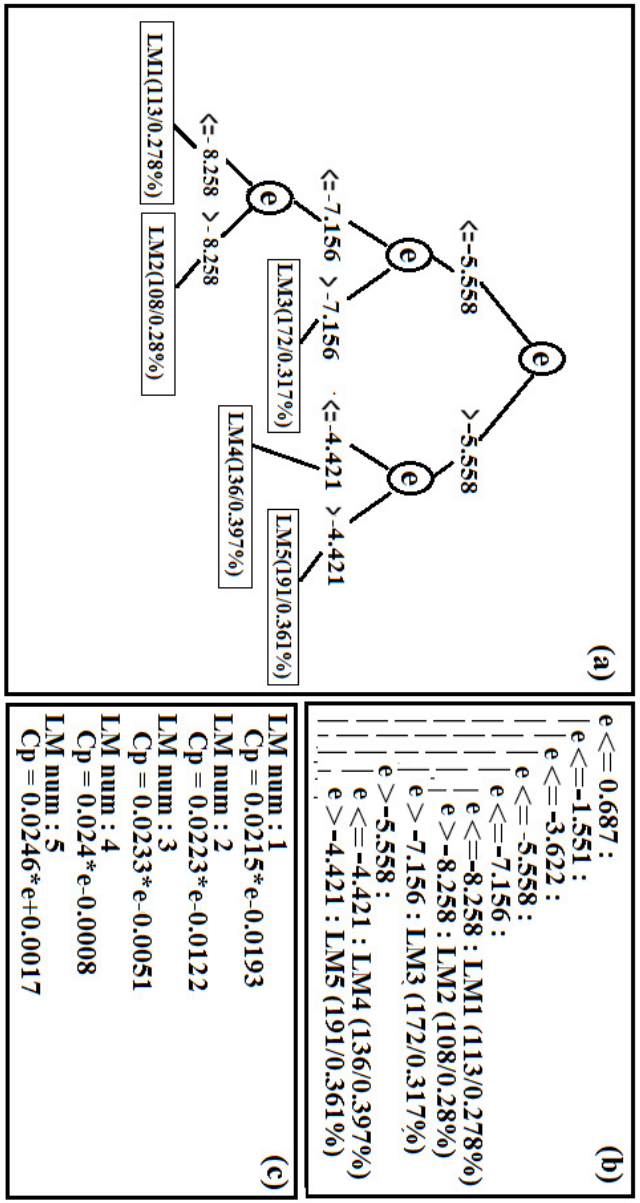
AIP Publishing

Journal of Renewable and Sustainable Energy

ACCEPTED MANUSCRIPT

This is the author's peer reviewed, accepted manuscript. However, the online version of record will be different from this version once it has been copyedited and typeset.

PLEASE CITE THIS ARTICLE AS DOI: 10.1063/5.0125713



AIP Publishing
Journal of Renewable and Sustainable Energy
ACCEPTED MANUSCRIPT
This is the author's peer reviewed, accepted manuscript. However, the online version of record will be different from this version once it has been copyedited and typeset.
PLEASE CITE THIS ARTICLE AS DOI: 10.1063/5.0125713

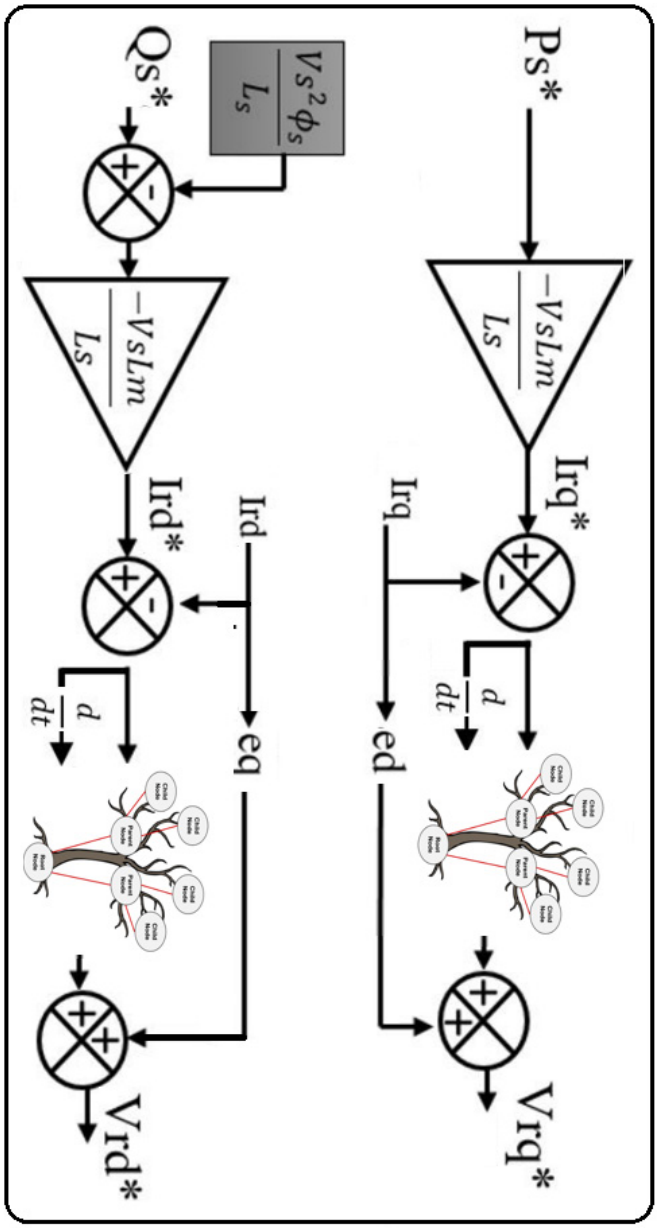
AIP Publishing

Journal of Renewable and Sustainable Energy

ACCEPTED MANUSCRIPT

This is the author's peer reviewed, accepted manuscript. However, the online version of record will be different from this version once it has been copyedited and typeset.

PLEASE CITE THIS ARTICLE AS DOI: 10.1063/5.0125713



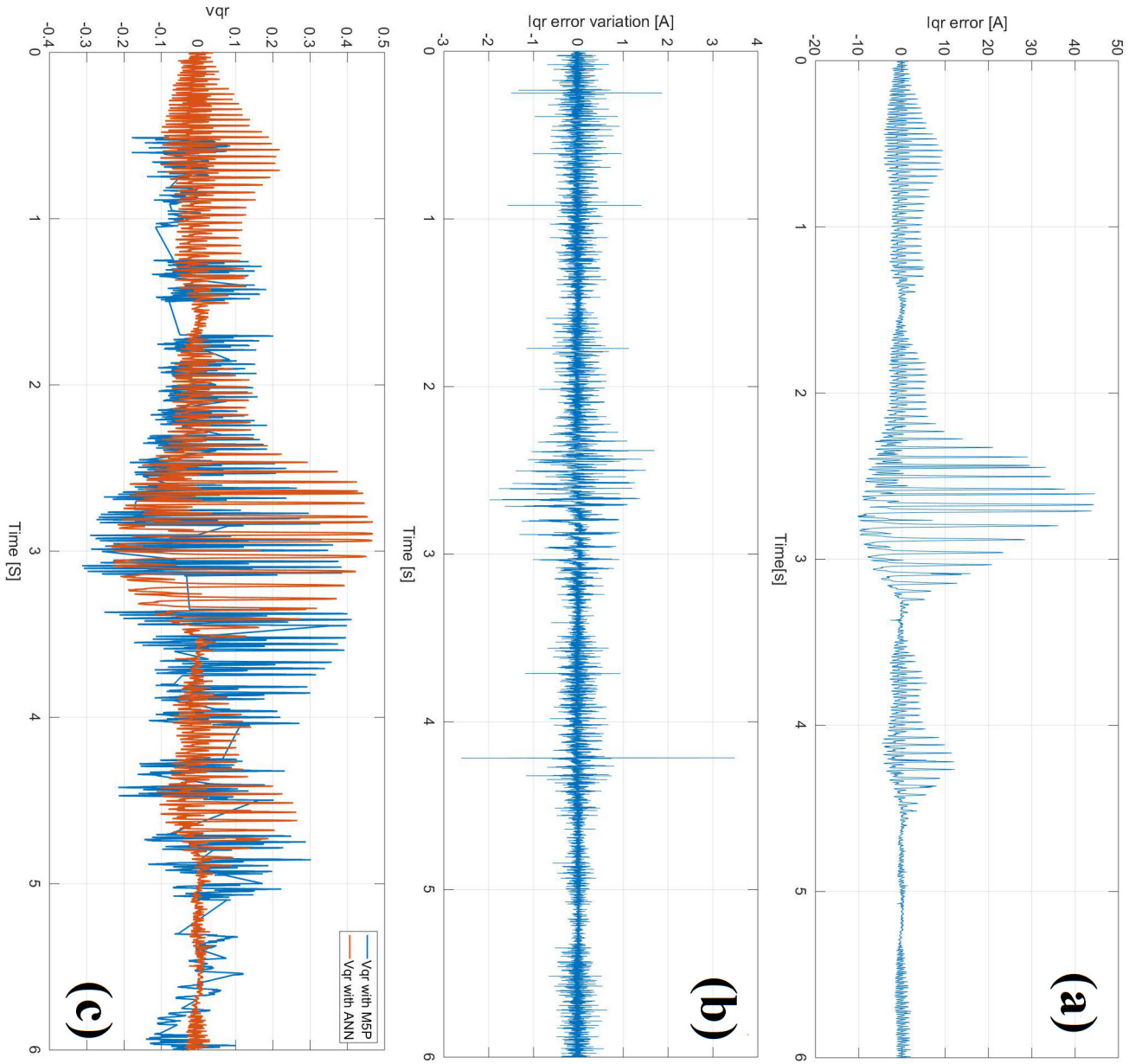
AIP Publishing

Journal of Renewable and Sustainable Energy

ACCEPTED MANUSCRIPT

This is the author's peer reviewed, accepted manuscript. However, the online version of record will be different from this version once it has been copyedited and typeset.

PLEASE CITE THIS ARTICLE AS DOI: 10.1063/5.0125713



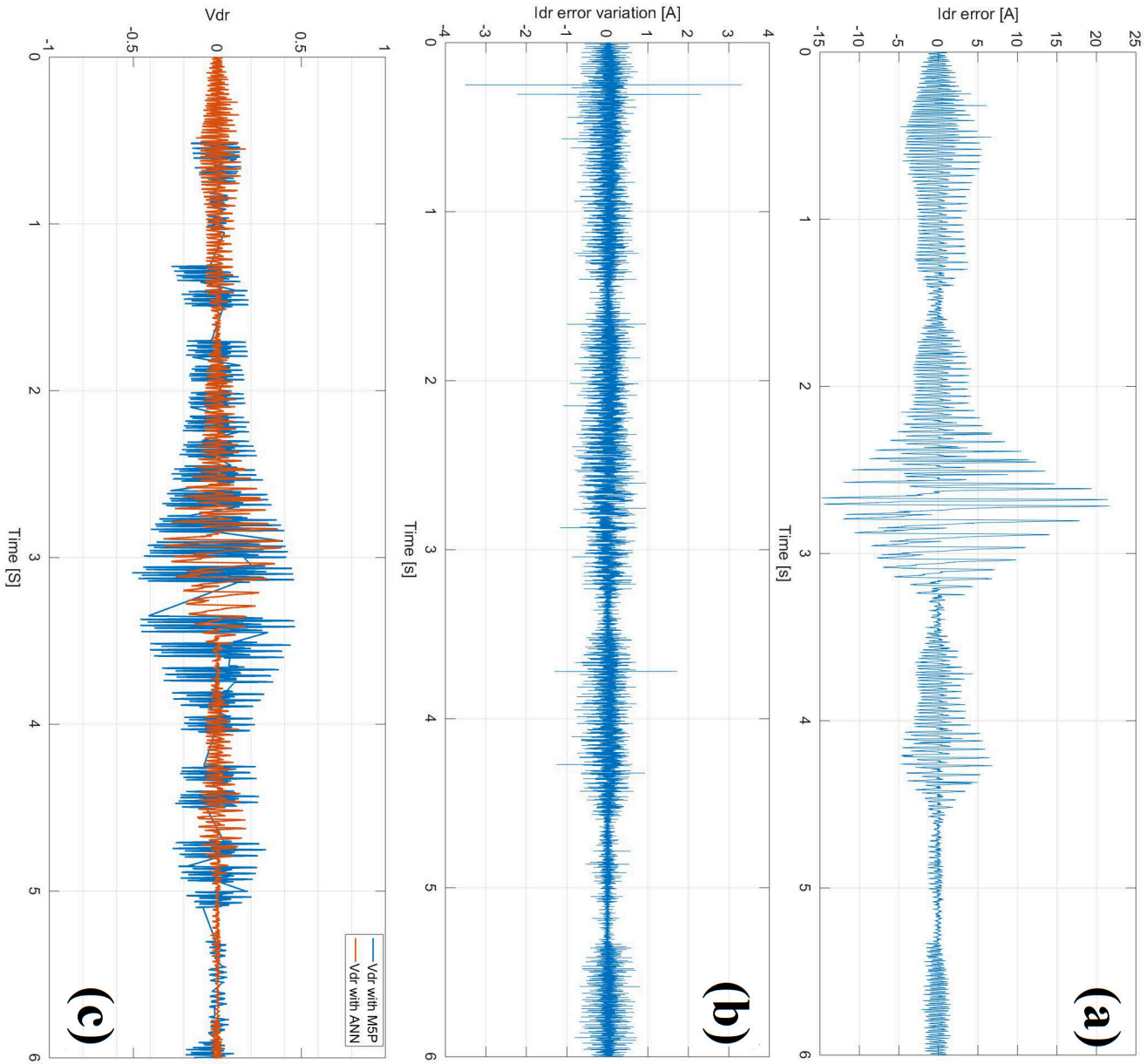
AIP Publishing

Journal of Renewable and Sustainable Energy

ACCEPTED MANUSCRIPT

This is the author's peer reviewed, accepted manuscript. However, the online version of record will be different from this version once it has been copyedited and typeset.

PLEASE CITE THIS ARTICLE AS DOI: 10.1063/5.0125713



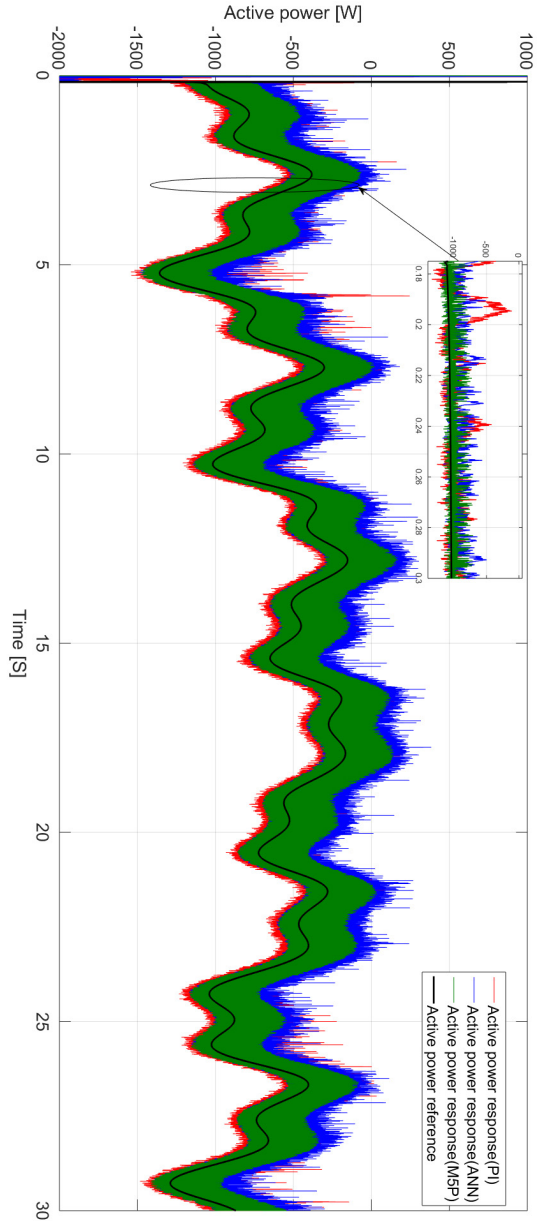
AIP Publishing

Journal of Renewable and Sustainable Energy

ACCEPTED MANUSCRIPT

This is the author's peer reviewed, accepted manuscript. However, the online version of record will be different from this version once it has been copyedited and typeset.

PLEASE CITE THIS ARTICLE AS DOI: 10.1063/5.0125713



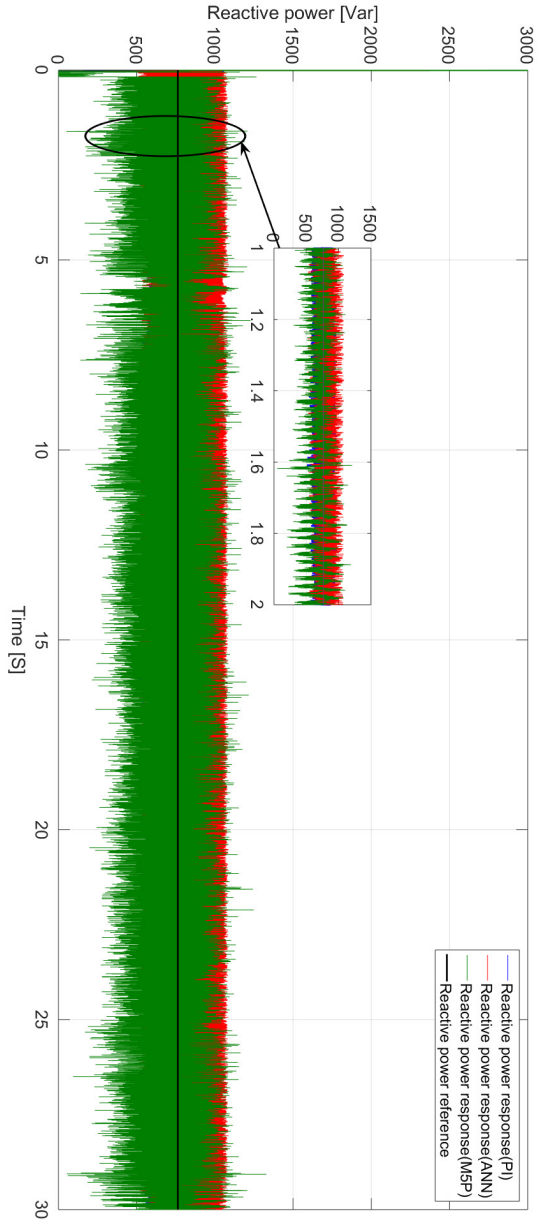
AIP Publishing

Journal of Renewable and Sustainable Energy

ACCEPTED MANUSCRIPT

This is the author's peer reviewed, accepted manuscript. However, the online version of record will be different from this version once it has been copyedited and typeset.

PLEASE CITE THIS ARTICLE AS DOI: 10.1063/5.0125713



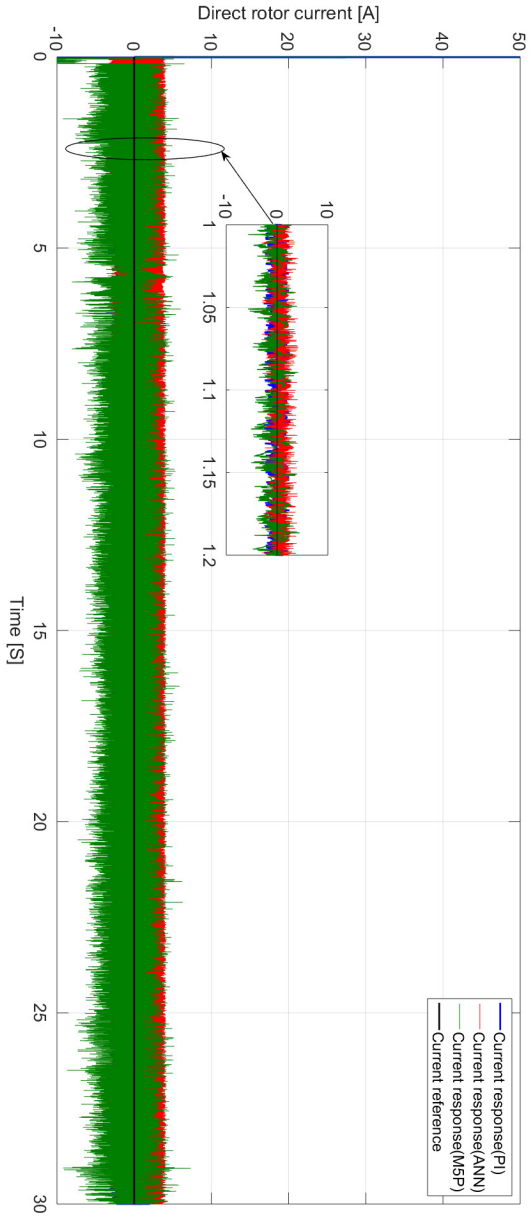
AIP Publishing

Journal of Renewable and Sustainable Energy

ACCEPTED MANUSCRIPT

This is the author's peer reviewed, accepted manuscript. However, the online version of record will be different from this version once it has been copyedited and typeset.

PLEASE CITE THIS ARTICLE AS DOI: 10.1063/5.0125713



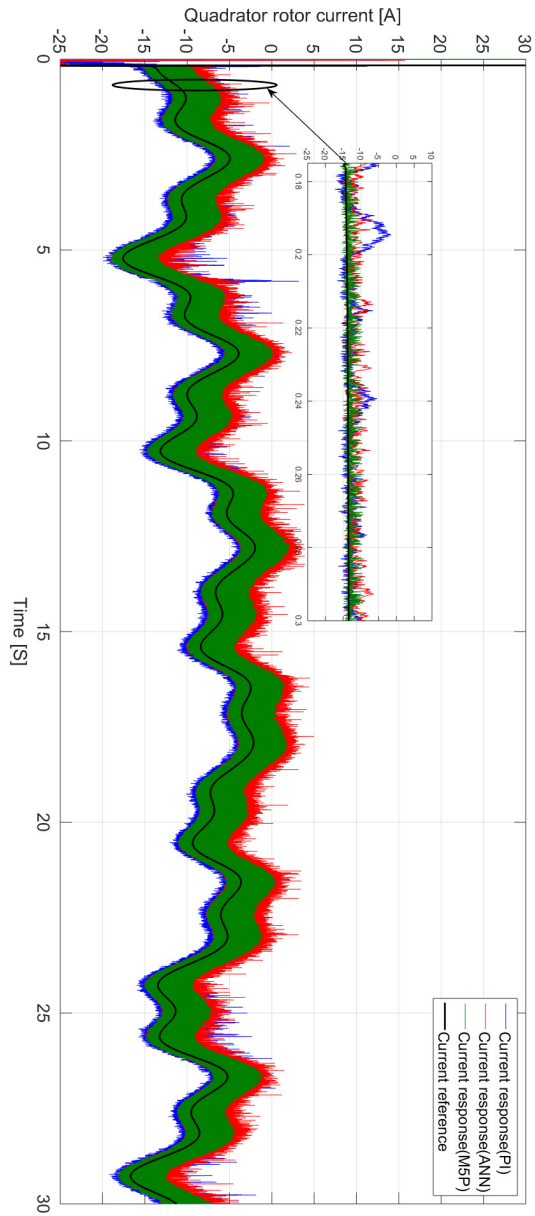
AIP Publishing

Journal of Renewable and Sustainable Energy

ACCEPTED MANUSCRIPT

This is the author's peer reviewed, accepted manuscript. However, the online version of record will be different from this version once it has been copyedited and typeset.

PLEASE CITE THIS ARTICLE AS DOI: 10.1063/5.0125713



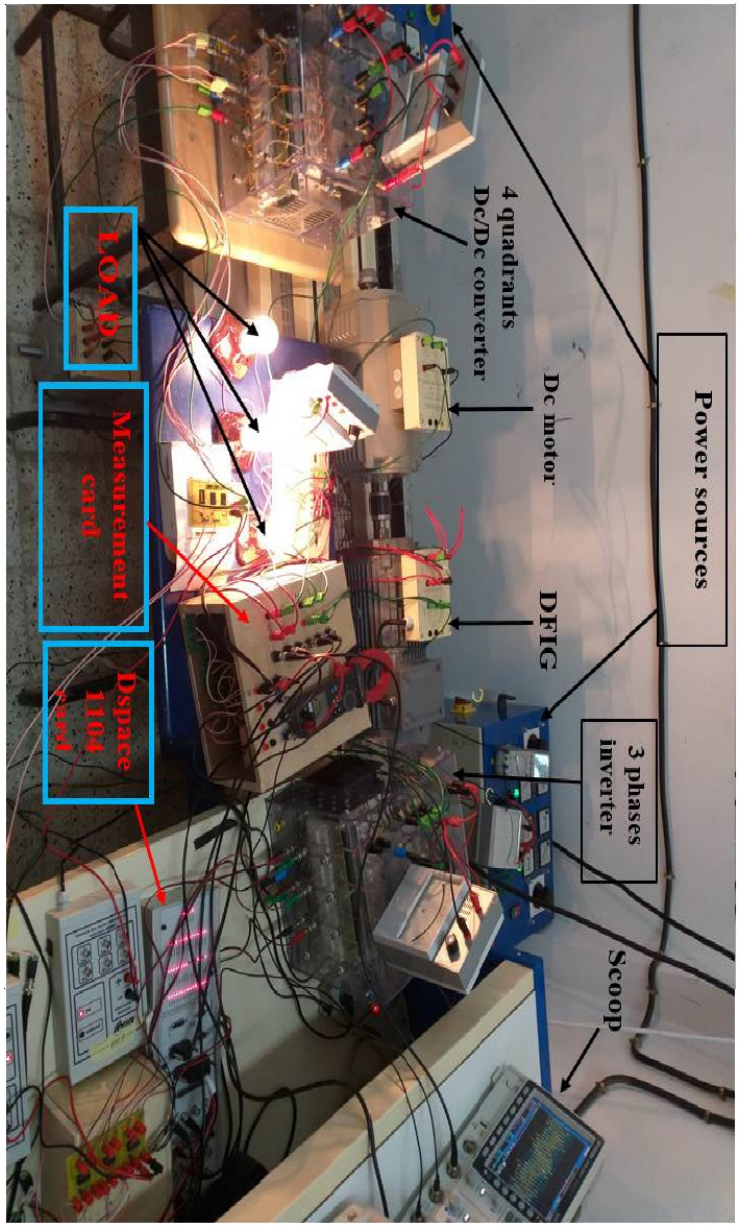
AIP Publishing

Journal of Renewable and Sustainable Energy

ACCEPTED MANUSCRIPT

This is the author's peer reviewed, accepted manuscript. However, the online version of record will be different from this version once it has been copyedited and typeset.

PLEASE CITE THIS ARTICLE AS DOI: 10.1063/5.0125713



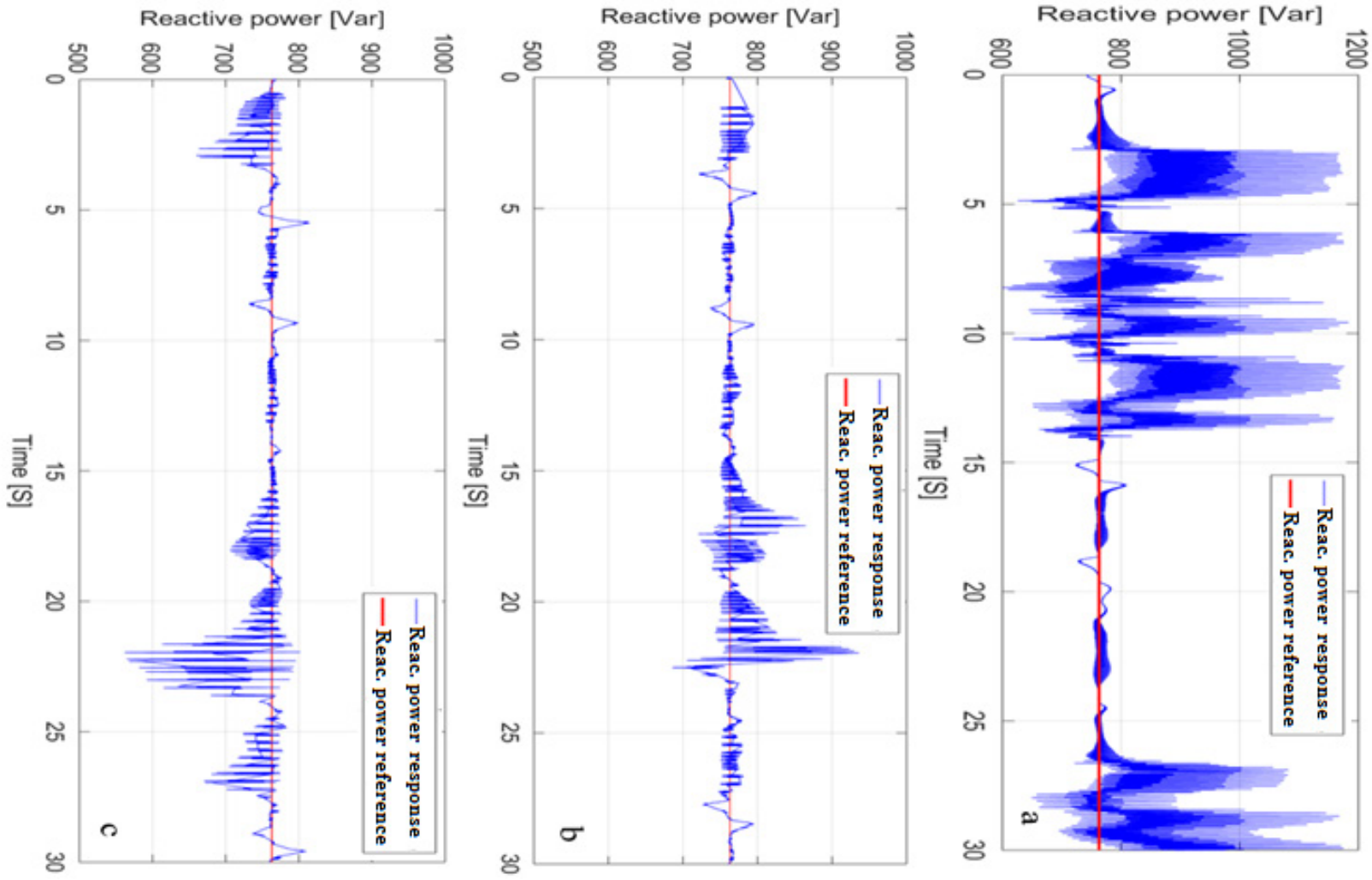
AIP Publishing

Journal of Renewable and Sustainable Energy

ACCEPTED MANUSCRIPT

This is the author's peer reviewed, accepted manuscript. However, the online version of record will be different from this version once it has been copyedited and typeset.

PLEASE CITE THIS ARTICLE AS DOI: 10.1063/5.0125713



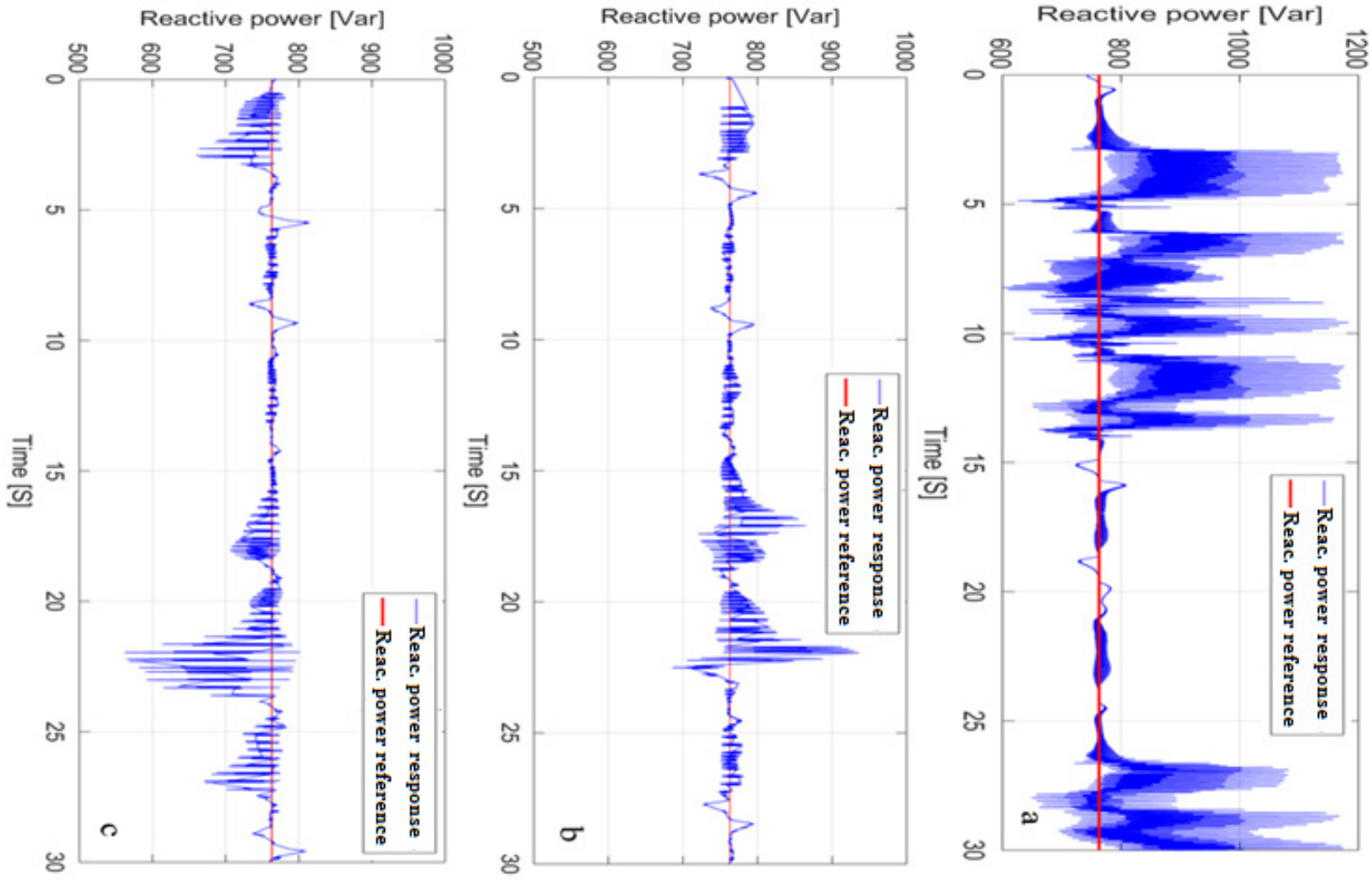
AIP Publishing

Journal of Renewable and Sustainable Energy

ACCEPTED MANUSCRIPT

This is the author's peer reviewed, accepted manuscript. However, the online version of record will be different from this version once it has been copyedited and typeset.

PLEASE CITE THIS ARTICLE AS DOI: 10.1063/5.0125713



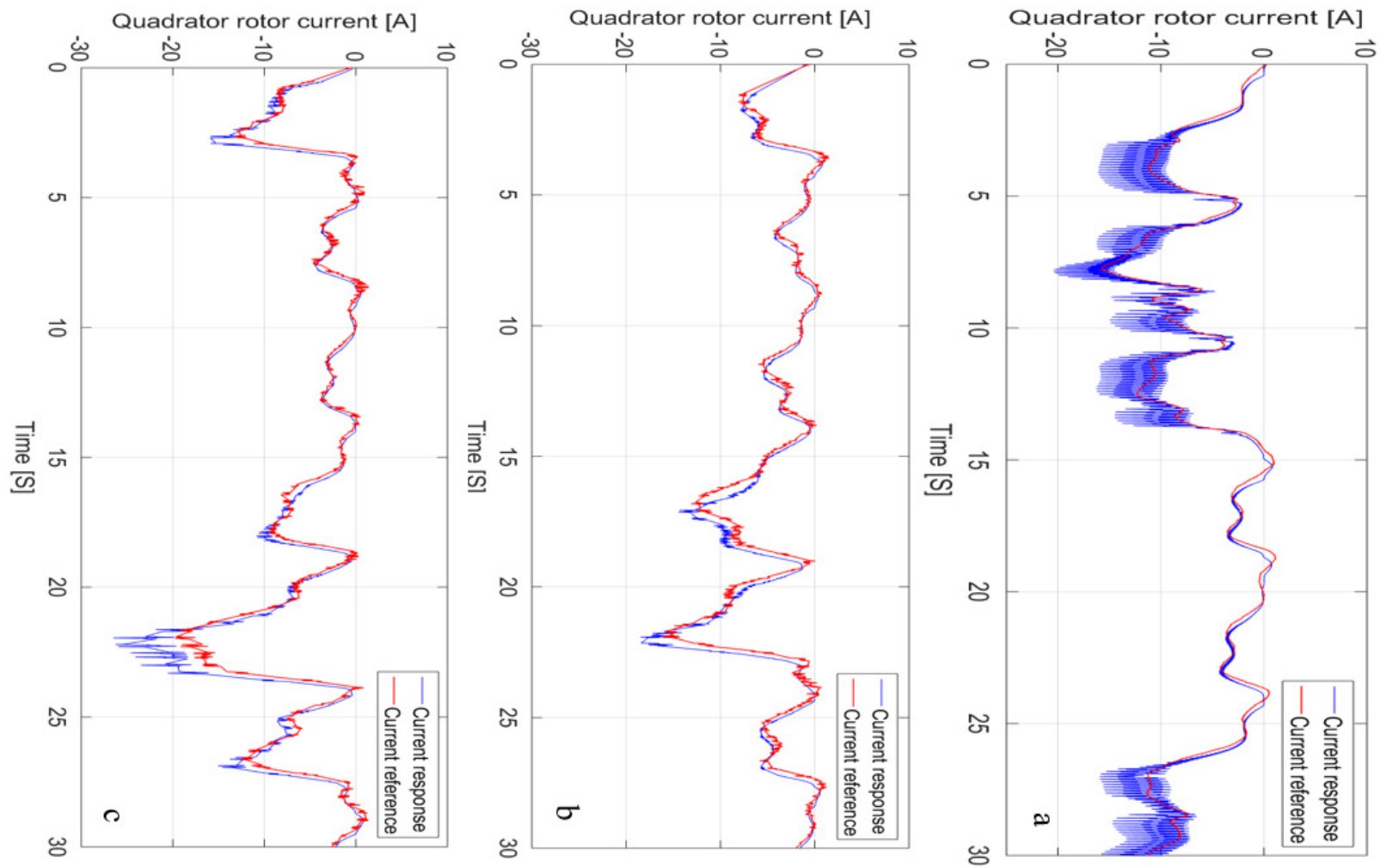
AIP Publishing

Journal of Renewable and Sustainable Energy

ACCEPTED MANUSCRIPT

This is the author's peer reviewed, accepted manuscript. However, the online version of record will be different from this version once it has been copyedited and typeset.

PLEASE CITE THIS ARTICLE AS DOI: 10.1063/5.0125713



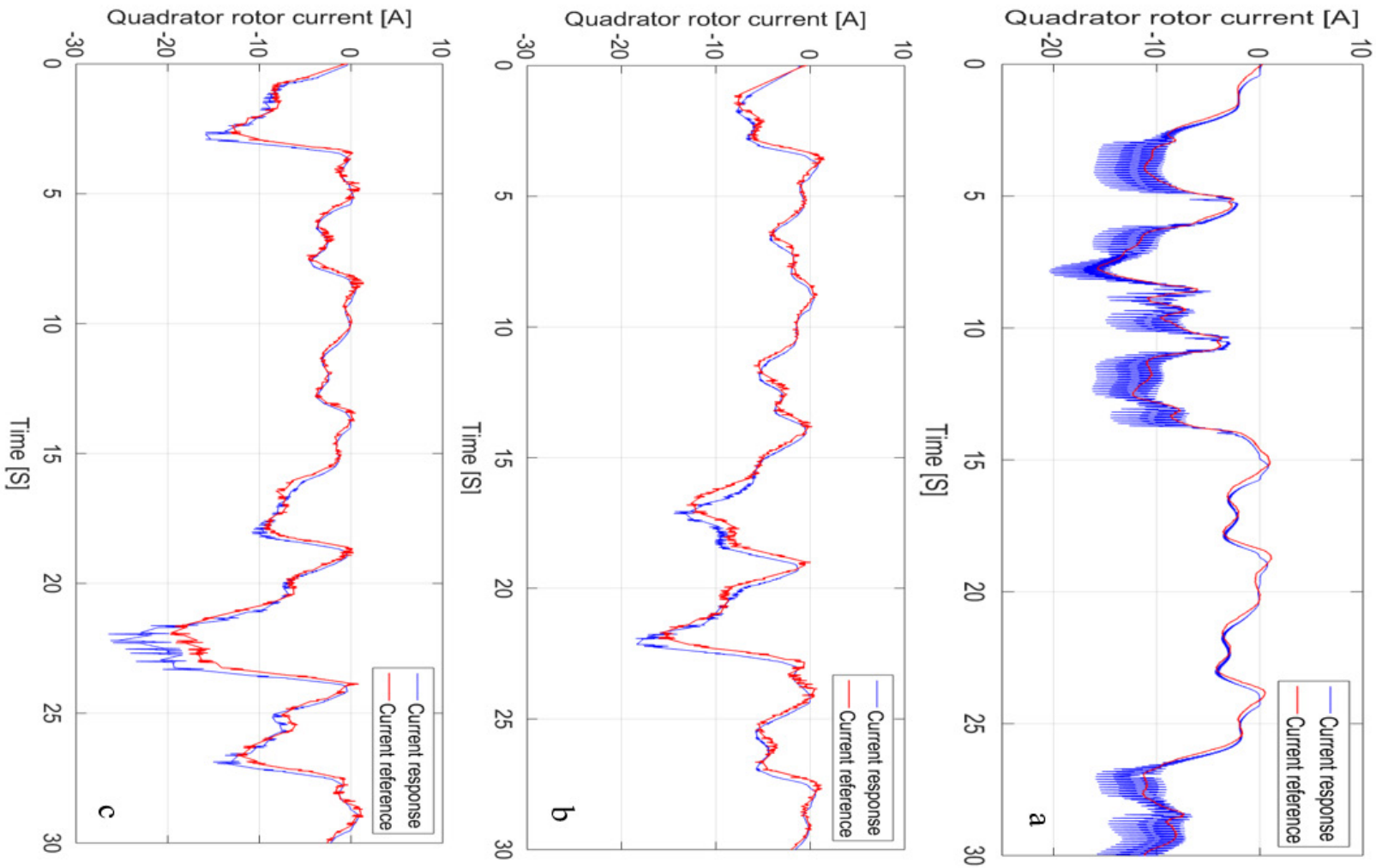
AIP Publishing

Journal of Renewable and Sustainable Energy

ACCEPTED MANUSCRIPT

This is the author's peer reviewed, accepted manuscript. However, the online version of record will be different from this version once it has been copyedited and typeset.

PLEASE CITE THIS ARTICLE AS DOI: 10.1063/5.0125713



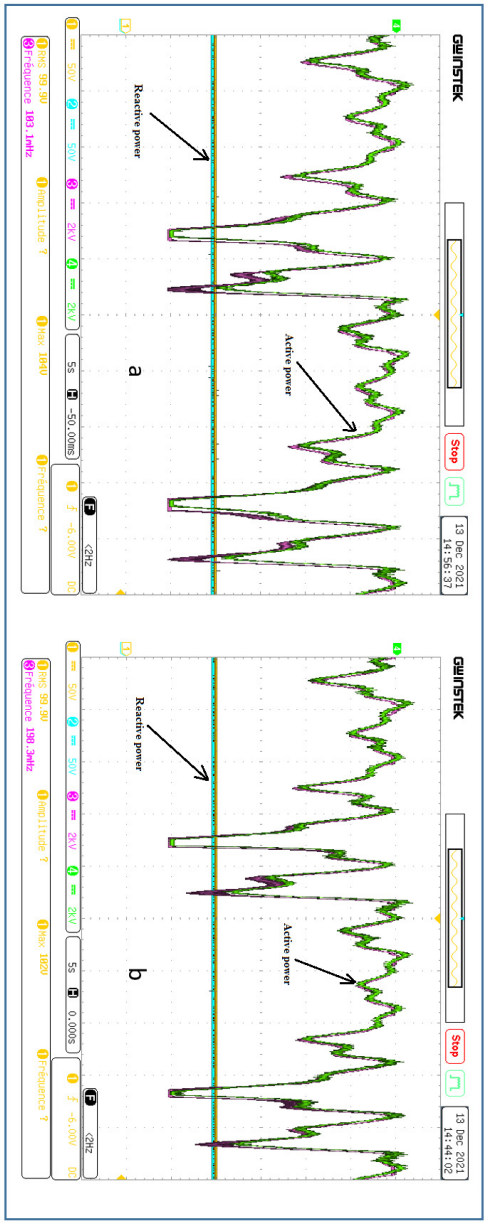
AIP Publishing

Journal of Renewable and Sustainable Energy

ACCEPTED MANUSCRIPT

This is the author's peer reviewed, accepted manuscript. However, the online version of record will be different from this version once it has been copyedited and typeset.

PLEASE CITE THIS ARTICLE AS DOI: 10.1063/5.0125713



AIP Publishing

Journal of Renewable and Sustainable Energy

ACCEPTED MANUSCRIPT

This is the author's peer reviewed, accepted manuscript. However, the online version of record will be different from this version once it has been copyedited and typeset.

PLEASE CITE THIS ARTICLE AS DOI: 10.1063/5.0125713

